



1 **Atmospheric processes of persistent organic pollutants over a remote lake of**  
2 **the central Tibetan Plateau: Implications for regional cycling**

3

4 Jiao Ren<sup>1,3</sup>, Xiaoping Wang<sup>1,2,\*</sup>, Chuanfei Wang<sup>1,2</sup>, Ping Gong<sup>1,2</sup>, and Tandong Yao<sup>1,2</sup>

5

6 <sup>1</sup>Key Laboratory of Tibetan Environment Changes and Land Surface Processes, Institute of Tibetan  
7 Plateau Research, Chinese Academy of Sciences, Beijing, 100101, China

8 <sup>2</sup>CAS Center for Excellence in Tibetan Plateau Earth Sciences, Beijing, 100101, China

9 <sup>3</sup>University of Chinese Academy of Sciences, Beijing 100049, China

10

11

12

13

14 **\* Corresponding author.**

15 (X. Wang)

16 E-mail: wangxp@itpcas.ac.cn

17 Tel: +86-10-84097120

18 Fax: +86-10-84097079



19 **Abstract**

20 Atmospheric processes (air-surface exchange, and atmospheric deposition and degradation) are crucial  
21 for understanding the global cycling and fate of persistent organic pollutants (POPs). However, such  
22 assessment over the Tibetan Plateau (TP) remains uncertain. More than 50% of the Chinese lakes are  
23 located on the TP, which exerts a remarkable influence on the regional water, energy, and chemical  
24 cycling. In this study, air and water samples were simultaneously collected in Nam Co, a large lake on  
25 the TP, to test whether the lake is a “secondary source” or “sink” of POPs. Lower concentrations of  
26 organochlorine pesticides (OCPs) and polychlorinated biphenyls (PCBs) were observed in the  
27 atmosphere and lake water of Nam Co, while the levels of polycyclic aromatic hydrocarbons (PAHs)  
28 were relatively higher. Results of fugacity ratios and chiral signatures both suggest that the lake acted as  
29 the net sink of atmospheric hexachlorocyclohexanes (HCHs), following their long-range transport  
30 driven by the Indian Monsoon. Different behaviors were observed in the PAHs, which primarily  
31 originated from local biomass burning. Acenaphthylene, acenaphthene, and fluorene showed  
32 volatilization from the lake to the atmosphere; while other PAHs were deposited into the lake due to the  
33 integrated deposition process (wet/dry and air-water gas deposition) and limited atmospheric  
34 degradation. As the dominant PAH compound, phenanthrene exhibited a seasonal reversal of air-water  
35 gas exchange, which was likely related to the melting of the lake ice in May. The annual input of HCHs  
36 from air to the entire lake area (2015 km<sup>2</sup>) was estimated as 1.9 kg year<sup>-1</sup>, while those estimated for  
37 PAHs can potentially reach up to 550 kg year<sup>-1</sup>. This study highlights the significance of PAH  
38 deposition on the regional carbon cycling in the oligotrophic lakes of the TP.



## 39 1. Introduction

40 Since the past century, large quantities of persistent organic pollutants (POPs), such as organochlorine  
41 pesticides (OCPs), polychlorinated biphenyls (PCBs), and polycyclic aromatic hydrocarbons (PAHs),  
42 have been discharged into the global environment. Soils, water bodies, and snow/ice are generally  
43 considered as reservoirs or sinks of these pollutants (Dalla Valle et al., 2005; Froescheis et al., 2000;  
44 Guglielmo et al., 2012). However, due to the influence of global warming (Komprda et al., 2013; Noyes  
45 et al., 2009), growing evidence indicates that POPs previously stored in reservoirs can be re-released  
46 back to the environment (Ma et al., 2011). For example, air-soil exchange of OCPs has showed the  
47 re-emission of OCPs from past contaminated soils in Europe (Ruzickova et al., 2008), North America  
48 (Kurt-Karakus et al., 2006), and India (Chakraborty et al., 2015). Modeling results have suggested that  
49 large parts of the global ocean have been losing dichlorodiphenyltrichloroethane (DDT) via  
50 volatilization (Stemmler and Lammel, 2009). In addition, air-sea exchange of PAHs has revealed that  
51 the seawater in the Mediterranean has turned into a temporary secondary source of PAHs, which is  
52 related to biomass burning in that region (Mulder et al., 2014). Moreover, melted sea glaciers have  
53 released large quantities of POPs back into the atmosphere in the polar regions, which has led to  
54 increased POP levels in air and water (Jantunen et al., 2008; Wong et al., 2011).

55 Similar to the polar regions, the Tibetan Plateau (TP) has been regarded as a “convergence” of POPs  
56 (Wang et al., 2016). Due to the continuous use of POPs in the surrounding countries and the “cold  
57 trapping” by the TP, the enrichment of POPs in the TP environment has been reported (Sheng et al.,  
58 2013; Wang et al., 2015). However, the TP has experienced great warming (Liu and Chen, 2000), and  
59 results of the air-soil exchange of POPs have indicated that the Tibetan soils are acting as a sink of DDT  
60 and higher molecular weight PAHs, but are a potential secondary source for hexachlorobenzene (HCB)  
61 and hexachlorocyclohexanes (HCHs) (Wang et al., 2014; Wang et al., 2012). This shows that the cold  
62 temperature over the TP might not be sufficient to trap volatile POPs. More studies on the air-surface  
63 exchange of POPs over the TP are therefore needed to test the role of the terrestrial and aquatic  
64 ecosystems of the TP in the regional cycling of POPs.

65 Known as “Asia’s water power”, the TP contains the headwaters of many major rivers in Asia, which  
66 provide water sources for about one-sixth of the world’s population (Yao et al., 2012). The TP also has  
67 large numbers of remote lakes that are important components of water bodies. Low temperature,  
68 oligotrophic conditions, and the long duration of ice-cover are distinct features of these lakes. Based on



69 the higher atmospheric concentrations of  $\alpha$ -HCH in summer, Xiao et al. (2010) deduced that these  
70 enhanced concentrations may be caused by the thawing of lake ice, which promotes the re-evaporation  
71 of  $\alpha$ -HCH. However, the study did not include measurements of POP levels in lake water or the  
72 corresponding air-water exchange analysis (Xiao et al., 2010). Therefore, it is still unclear whether the  
73 lake water of the TP is the secondary source of a large number of POPs. Furthermore, biomass burning  
74 is a widespread activity over the TP (Hu et al., 2015). A recent study demonstrated that the locally  
75 sourced biomass combustion particles contributed substantially to the black carbon (BC) loading of the  
76 TP glacier (Li et al., 2016). Given that PAHs and BC both originate from incomplete combustion of  
77 biomass, regional air-water exchange of PAHs would also contribute to the overall air-surface exchange  
78 of carbon.

79 We therefore conducted air and water sampling in a remote lake on the TP, and assessed the air-water  
80 gas exchange, and the dry and wet deposition processes of OCPs, PCBs, and PAHs. The aims of this  
81 study were to ascertain whether the Tibetan lake represents a secondary source of POPs, to investigate  
82 the influence of seasonal lake ice melting on the gas exchange of different POPs, and to estimate the  
83 contribution of PAH exchange to the lake carbon budget.

## 84 **2. Materials and methods**

### 85 **2.1 Site description**

86 Nam Co Lake (30°30′–30°56′N, 90°16′–91°01′E, 4718 m) is located in the north of the  
87 Nyainqentanglha Mountains, on the central TP (Figure 1). It is the second largest lake in Tibet with an  
88 area of 2015 km<sup>2</sup> and a maximum depth exceeding 90 m (Wang et al., 2009). The climate of Nam Co is  
89 relatively cold and windy with an annual average temperature of ~0 °C and an annual wind speed of ~4  
90 m/s. The regional climate also has large seasonal variation: the Indian Monsoon dominates summer  
91 (May to September) and the westerlies control winter climate (October to April) [see the Supplement  
92 (S), Figure S1]. High temperatures and precipitation are usually observed in summer (Figure S2), and  
93 the lake begins to thaw from the beginning of May and melts completely by the end of May, which  
94 coincides with the onset of the Indian Monsoon. During the winter, the lake is covered by ice due to the  
95 subzero temperatures (Figure S2) and maximum instantaneous wind speeds reaching up to 9.9 m/s.

96 The dominant land cover in Nam Co is alpine steppe and meadow, and the local residents herd yak and  
97 sheep that graze around the lake. Biomass burning occurs for heating, cooking, transport, and religious  
98 reasons. Near the southeastern shore, the Nam Co Monitoring and Research Station for Multisphere



99 Interactions (NCMORS) is operated by the Chinese Academy of Sciences (Figure 1b). This station not  
100 only facilitates the consecutive collection of field samples used in the current study, but also provides  
101 local meteorological parameters for flux calculations.

## 102 **2.2 Air and water sampling**

103 An active air sampler (AAS) was deployed on the roof of NCMORS (Figure 1b) and the air monitoring  
104 was conducted for two consecutive years from September 2012 to September 2014. The flow rate of  
105 AAS was  $60 \text{ L min}^{-1}$  and the air samples were collected every 2 weeks with a volume of approximately  
106  $600 \text{ m}^3$  for each sample. The air stream passes first through glass fiber filters (GFFs  $0.7 \mu\text{m}$ , Whatman)  
107 to collect the total suspended particulates (TSP) and then through polyurethane foam (PUF,  $7.5 \times 6 \text{ cm}$   
108 diameter) to retain the POPs in gas phase. In total, 47 air samples were collected. Details regarding the  
109 sampling period, average air temperature, and wind speed are given in Table S1. All harvested PUF and  
110 GFFs were stored at  $-20 \text{ }^\circ\text{C}$  until extraction.

111 To determine the POP levels in water, two sampling programs were conducted. First, 15 sites around the  
112 Nam Co Lake (surface lake water, 0–1 m depth) were selected to obtain the spatial distribution of POPs  
113 in lake water (Figure 1b), which provides a direct over-view of POP contamination over the lake.  
114 Second, monthly water samples were collected at a site close to NCMORS (Figure 1b) from May to  
115 September, 2014 (water samples were not obtained during winter due to the ice cover). This provided  
116 information regarding temporal variations in POP levels, isomer ratios, and the enantiomeric fraction in  
117 lake water. Furthermore, coupled with the monthly average air concentrations of individual POPs  
118 obtained, this allowed us to investigate the air-water gas exchange of POPs (direction, flux, and monthly  
119 variations).

120 Water samples (200 L) were filtered with GFFs to obtain the total suspended particulate matter (SPM),  
121 and then pumped through an XAD-2 resin column to collect the dissolved phase compounds. For each  
122 sampling month, triplicate samples were collected. In total, 15 samples for the spatial study and 15  
123 samples for the temporal study were collected. XAD columns were kept at  $4 \text{ }^\circ\text{C}$  until extraction. The  
124 lake water properties (salinity and temperature) are provided in Table S2.

## 125 **2.3 Sample extraction and analysis**

126 The chemical extraction and cleanup methods are detailed in Text S1 for each sample type [air (PUF  
127 plug), TSP, water (XAD column), and SPM]. POPs were analyzed on a gas chromatograph with an  
128 ion-trap mass spectrometer (GC-MS, Finnigan Trace GC/PolarisQ) operating under MS–MS mode.



129 More information on the chromatographic conditions is given in Text S2. The target compounds are as  
130 follows: HCHs (including  $\alpha$ -HCH,  $\beta$ -HCH, and  $\gamma$ -HCH), HCB, DDTs (*o,p'*-DDE, *p,p'*-DDE, *o,p'*-DDT,  
131 and *p,p'*-DDT), PCBs (PCB 28, PCB 52, PCB 101, PCB 138, PCB 153, and PCB 180), and 15 priority  
132 PAHs listed by the United States Environment Protection Agency (USEPA, without naphthalene),  
133 including acenaphthylene (Acel), acenaphthene (Ace), fluorene (Flu), phenanthrene (Phe), anthracene  
134 (Ant), fluoranthene (Fla), pyrene (Pyr), benz[a]anthracene (BaA), chrysene (Chr), benzo[b]fluoranthene  
135 (Bbf), benzo[k]fluoranthene (Bkf), benzo[a]pyrene (BaP), dibenz[a, h]anthracene (DahA), benzo[g, h,  
136 i]perylene (BghiP), and indeno[1,2,3-cd]pyrene (IcdP). Enantiomers of  $\alpha$ -HCH were determined with a  
137 BGB-172 chiral column (see Text S2 for details). The chiral signature of  $\alpha$ -HCH is expressed using the  
138 enantiomeric fraction (EF), which is equal to the ratio of peak areas of the (+)/[(+) + (-)] (Harner et al.,  
139 2000).

#### 140 **2.4 Quality assurance/quality control (QA/QC)**

141 All analytical procedures were monitored using strict QA/QC measures. Prior to sampling, PUF and  
142 XAD resin were pre-cleaned using dichloromethane (DCM) for 16 h and GFFs were baked at 450 °C for  
143 4 h. Six PUF field blanks, three XAD field blanks, and six procedural blanks were prepared; HCB, Phe,  
144 Ant, Fla, and Pyr were detected in the field blanks (Table S3). The definitions of the method detection  
145 limits (MDLs) are described in Text S3, and the derived MDLs are given in Table S4. The breakthrough  
146 of PUF plugs was checked in eleven split PUFs, and the results show that the individual POPs in the  
147 second half varied from 8% to 23% (Table S5), indicating good retention capacity. Certified surrogate  
148 standards (from Dr. Ehrenstorfer GmbH, Germany) were analyzed alongside each sample. The  
149 recoveries ranged from 71% to 94% for PCB 30, 79% to 105% for Mirex, and 65% to 92% for  
150 perylene-D12. The reported concentrations were subtracted by mean blanks but not corrected for  
151 recoveries. To check the reproducibility of the chiral analysis, the racemic standard of  $\alpha$ -HCH was  
152 injected repeatedly and its average EF value was  $0.499 \pm 0.001$  ( $n = 5$ ).

#### 153 **2.5 Calculations of air-water gas exchange**

154 Concurrent air and water samples were used to assess the status of air-water gas exchange in Nam Co  
155 Lake. The gas exchange direction can be determined by the ratio of fugacity in water ( $f_w$ ) and air ( $f_a$ ),  
156 giving the fugacity ratio ( $f_w/f_a$ ) (Jantunen et al., 2015):

$$157 \quad f_a = C_G RT_a \quad (1)$$

$$158 \quad f_w = C_w H \quad (2)$$



159 where  $C_G$  and  $C_w$  are the gaseous and dissolved concentrations of target compounds in air and water,  
 160 respectively,  $R$  is the gas constant ( $8.314 \text{ Pa m}^3 \text{ mol}^{-1} \text{ K}^{-1}$ ),  $T_a$  (K) is the air temperature, and  $H$  ( $\text{Pa m}^3$   
 161  $\text{mol}^{-1}$ ) is the Henry's law constant. According to the method reported by Ruge et al. (2015), the POP  
 162 concentrations retained by XAD were calibrated to derive the true freely dissolved POP concentrations  
 163 in water ( $C_w$ , Text S4).  $H$  values were adjusted for the real water temperature and salinity of Nam Co by  
 164 the procedure described in Text S5 (Cetin et al., 2006; Ma et al., 2010). Ratios of  $f_w/f_a > 1$  generally  
 165 indicate volatilization,  $< 1$  indicates deposition, and equilibrium is reached at 1. Due to uncertainties, a  
 166 significant deviation from equilibrium cannot be assessed in a range of 0.3–3 (Lohmann et al., 2009;  
 167 Xie et al., 2011).

168 Net fluxes of air-water gas exchange ( $F_{AW}$ ,  $\text{ng m}^{-2} \text{ day}^{-1}$ ) were quantified using the Whitman two-film  
 169 model, which has been used in many previous studies (Iwata et al., 1993; Khairy et al., 2014):

$$170 \quad F_{AW} = K_{ol} (C_w - C_G R T_a / H) \quad (3)$$

171 where  $K_{ol}$  ( $\text{m s}^{-1}$ ) is the overall mass transfer coefficient, which contains contributions from the mass  
 172 transfer coefficients of the water and air layers,  $K_w$  and  $K_a$ , respectively. They are related to the wind  
 173 speed and compound-specific molecular diffusivity; a detailed calculation is presented in Text S6.  
 174 Positive flux values indicate net volatilization, and negative values indicate net deposition.

## 175 2.6 Estimation of dry and wet deposition fluxes

176 In addition to the gas exchange, dry and wet deposition are also important processes that control the  
 177 input of POPs from air to lake. Dry deposition fluxes ( $F_{DD}$ ,  $\text{ng m}^{-2} \text{ day}^{-1}$ ) of atmospheric  
 178 particulate-phase POPs can be calculated using (Gonzalez-Gaya et al., 2016) the following equation:

$$179 \quad F_{DD} = 0.864 V_D C_P \quad (4)$$

180 where  $V_D$  ( $\text{cm s}^{-1}$ ) is the compound specific deposition velocity,  $C_P$  is the measured POPs concentrations  
 181 in TSP ( $\text{pg m}^{-3}$ ), and 0.864 is a unit conversion factor.  $V_D$  for each sampling period and compound was  
 182 estimated using an empirical equation derived by Gonzalez-Gaya et al. (2014):

$$183 \quad \log(V_D) = -0.261 \log(P_L) + 0.387 U_{10} Chl_s - 3.082 \quad (5)$$

184 where  $P_L$  (Pa) is subcooled liquid vapor pressure of chemicals that was corrected to the local  
 185 temperature using the equations given in Table S6,  $U_{10}$  ( $\text{m s}^{-1}$ ) is wind speed at 10 m height converted  
 186 from the field-measured wind speed at 1.5 m (Table S1), and  $Chl_s$  is the surface chlorophyll  
 187 concentration ( $\text{mg m}^{-3}$ , Liu et al., 2010).



188 Wet deposition fluxes ( $F_{WD}$ ,  $\text{ng m}^{-2} \text{day}^{-1}$ ) were estimated using the method established by Jurado et al.  
189 (2005):

$$190 \quad F_{WD} = P(W_G C_G + W_P C_P) \quad (6)$$

191 where  $P$  is precipitation depth per day ( $\text{m d}^{-1}$ ) derived from the data recorded in the NCMORS, and  $W_G$   
192 and  $W_P$  are the gas and particle washout ratios, respectively. Assuming that equilibrium is attained  
193 between the gas phase and the dissolved phase in a raindrop/snow,  $W_G$  was estimated by (Wania et al.,  
194 1998a):

$$195 \quad W_G = RT_a/H \quad (7)$$

196 In contrast to gas scavenging, particle scavenging by precipitation is a complex process controlled by  
197 meteorological conditions and the properties of the aerosols. Thus, the recommended values of  $W_P$  in  
198 literature (Franz and Eisenreich, 1998; Jurado et al., 2005) were adopted to consider the different  
199 particle scavenging by rain and snow.

### 200 **3. Results and discussion**

201 We determined the POP concentrations in air, TSP, water, and SPM separately; the full data sets are  
202 listed in Tables S7-S10. OCPs and PCBs were rarely detected in TSP (Table S8), and were therefore not  
203 considered in further discussion. Comparisons between the data from this study and previously  
204 published values for the TP and other remote regions are presented in Tables S11-S14.

#### 205 **3.1 Levels of POPs in air and water at Nam Co**

206 The concentrations of POPs in the atmosphere and TSP in Nam Co are summarized in Figure 2 using  
207 box-and-whisker plots. Among the OCPs, HCB was the dominant chemical with an average  
208 concentration of  $20 \text{ pg m}^{-3}$  (Figure 2a), which was two times higher than that reported for southeastern  
209 TP (Sheng et al., 2013) and Mt. Everest (Li et al., 2006) (Table S11), but lower than the values in the  
210 Rocky Mountains ( $42 \text{ pg m}^{-3}$ , Wilkinson et al., 2005) and the Arctic ( $64 \text{ pg m}^{-3}$ , Su et al., 2006). The  
211  $\alpha$ -HCH (average  $4.0 \text{ pg m}^{-3}$ ) and  $\gamma$ -HCH ( $2.1 \text{ pg m}^{-3}$ ) values in this study were much lower than those  
212 measured using a flow-through sampler (FTS) during 2006 to 2008 ( $48.7$  and  $7.9 \text{ pg m}^{-3}$ , respectively)  
213 (Xiao et al., 2010). The DDT concentrations in the current study ( $0.8$ - $46.4 \text{ pg m}^{-3}$ ) were lower than  
214 those observed for Lulang in southeastern TP (Table S11) (Sheng et al., 2013), which is the entrance of  
215 the Indian Monsoon. In spite of this, the levels of DDTs were still one order of magnitude higher than  
216 those for the Arctic (Table S11) (Su et al., 2008). Lower concentrations of  $\sum_6\text{PCBs}$  were also detected  
217 in air with an average value of  $2.5 \text{ pg m}^{-3}$ .





218 The sum concentrations of  $\sum_{15}$ PAHs in the atmosphere ranged from 0.5–13 and 0.1–3.4 ng m<sup>-3</sup> in the  
219 gaseous and particulate phases, with averages of 2.2 and 0.6 ng m<sup>-3</sup>, respectively. The 3- and 4-ring  
220 PAHs were predominant in both phases, including Phe, Flu, Fla, and Pyr (Figure 2b and 2c). The PAH  
221 levels in Nam Co were one order of magnitude lower than those reported for Lhasa (35.7 ng m<sup>-3</sup>, Table  
222 S12), which is the capital city of Tibet with a large population, extensive tourism, and abundant  
223 religious activities (Gong et al., 2011). Compared with background levels in other regions of the world  
224 (Table S12), the PAHs in this study were comparable to the levels in Arctic air (Ding et al., 2007), but  
225 significantly higher than those from European mountainous regions (Fernandez et al., 2002).

226 In the lake water, the average dissolved concentrations of  $\alpha$ -HCH,  $\beta$ -HCH,  $\gamma$ -HCH, HCB, and PCB 28  
227 were 9.9, 85.2, 7.0, 7.6, and 1.9 pg L<sup>-1</sup>, respectively; while DDT-related compounds were below MDLs  
228 in most cases for both dissolved and SPM phases (Table S9 and S10). The current measured HCH  
229 concentrations were approximately two orders of magnitude lower than values reported for the  
230 Yamdrok and Co Ngoin Lake in 2002 (Table S13) (Zhang et al., 2003). Two possible reasons for this  
231 discrepancy are: i) the inter-annual variation of POPs, i.e., the concentrations declined rapidly since  
232 2002; and ii) the uncertainties caused by analytical and instrumental method (electron capture detector  
233 in Zhang et al. (2003) study and the MS detector in the current study). From a global perspective, the  
234 HCH concentrations obtained by this study were overall lower than those in European mountain lakes  
235 (Table S13). DDT class chemicals were rarely detected and only PCB 28 could be quantified in the  
236 Nam Co lake water. These features combined with the low levels of HCHs suggest that the POP levels  
237 in Nam Co lake water were close to the values reported for ocean waters, such as, the North Atlantic  
238 and Arctic oceans (with DDTs and PCBs mostly below the detection level, or <1 pg L<sup>-1</sup>) (Gioia et al.,  
239 2008; Lohmann et al., 2009). By contrast, high levels of PAHs were found in the Nam Co lake water,  
240 ranging from 6.9 to 83.6 and 1.7 to 28 ng L<sup>-1</sup> for the dissolved and SPM phases, respectively. The  
241 dissolved  $\sum_{15}$ PAH levels were one order of magnitude higher than those reported for Himalayan  
242 high-altitude lakes in Nepal (Table S14) (Guzzella et al., 2011) and the Great Lakes (Table S14) (Venier  
243 et al., 2014), and two orders of magnitude greater than values for open oceans (Table S14) (Ma et al.,  
244 2013) and European mountain lakes (Table S14) (Vilanova et al., 2001).

### 245 3.2 Possible sources

246 Long range atmospheric transport (LRAT) is considered an important source contributing to the  
247 occurrence of POPs in remote environments (Dalla Valle et al., 2005). Considering that the prevailing



248 climate system operating over Nam Co in summer is the Indian Monsoon, if the seasonal pattern of a  
249 chemical is similar to that of the monsoon, monsoon transport may therefore be the source of POPs in  
250 Nam Co air. Thus, the interrelationship between monsoon intensity (Indian Monsoon Index, IMI,  $W m^{-2}$ )  
251 and POP concentrations was investigated (Figure 3). Figure 3 shows that  $\alpha$ -HCH and *o,p'*-DDT  
252 displayed synchronous seasonal variation with the IMI. This suggests that monsoon transport was the  
253 principal reason for the occurrence of OCPs in the Nam Co atmosphere. In addition, isomer ratios can  
254 provide insight on the source and fate of the POPs. In this study, we found that the isomer ratios of  
255 *p,p'*-DDT to *p,p'*-DDE were broadly in agreement with those found for the source regions of India and  
256 the Bay of Bengal (Table S15) (Gioia et al., 2012; Zhang et al., 2008). Similar to other remote regions,  
257 such as, the Arctic (Hung et al., 2010), Antarctic (Baek et al., 2011), Rocky Mountains (Daly et al.,  
258 2007), and southeastern TP (Sheng et al., 2013), in which LRAT is the primary transport mode of POPs,  
259 the dominance of  $\alpha$ - to  $\gamma$ -HCH was observed in the Nam Co atmosphere (Table S15). Results of isomer  
260 ratios associated with the seasonal variations supported the interpretation that OCPs in the Nam Co  
261 atmosphere had undergone LRAT. In contrast to OCPs, neither the gaseous nor the particulate phases of  
262 PAHs showed a clear and consistent seasonal variation during the two years of air monitoring (Figure  
263 S3), which is likely because there were primary emissions of PAHs surrounding the Nam Co region.

264 Apart from the seasonal trends, spatial distribution patterns can also provide valuable information on  
265 POP sources. The spatial distributions of POPs in the surface water across the Nam Co Lake are  
266 presented in Figure 4. First, HCHs showed a uniform distribution (Figure 4) without significant  
267 differences among the different regions of the lake (Table S16). The even distribution of HCHs in the  
268 water was most likely caused by the LRAT origins and relatively higher water solubility. Second,  
269 relatively high levels of HCB and PAHs occurred in water from the northwestern and eastern parts of  
270 the lake (Table S16 and Figure 4). The elevated HCB and PAHs in these regions were likely related to  
271 anthropogenic activity in the vicinity. As shown in Figure 1b, two townships (Baoji and Namco), which  
272 have the highest population around Nam Co Lake, are located in the northwestern and eastern corners of  
273 the lake. Following a traditional lifestyle, the residents use large amounts of local biomass (mostly yak  
274 dung) for cooking and heating (Xiao et al., 2015). High PAH concentrations have been reported in local  
275 Tibetan tents that were emitted mainly from burning yak dung (Li et al., 2012). A ratio of  
276  $BaA/(BaA+Chr) = 0.33$  was recommended as a specific diagnostic fingerprint for yak dung combustion  
277 (Li et al., 2012). The  $BaA/(BaA+Chr)$  ratios observed in our study ( $0.27 \pm 0.08$  for air and  $0.24 \pm 0.10$  for  
278 water) were in good agreement with this diagnostic ratio. This suggests that local combustion emission



279 is likely the source of PAHs in Nam Co. With the exception of PAHs, biomass combustion can also  
280 produce HCB (Bailey, 2001), which may be the reason for the higher HCB concentrations occurring  
281 around the townships. The spatial distribution of POPs in the Nam Co lake water highlights the  
282 important contribution of local sources for PAHs and HCB.

### 283 3.3 LRAT versus re-volatilization

284 From the above results, we found that LRAT is a key factor that determines the seasonality of the  
285 atmospheric HCHs and DDTs in Nam Co (higher concentrations occurred in summer). However, high  
286 temperatures generally occur during summer, which may promote the evaporation of chemicals from  
287 local surfaces (e.g., soils and water bodies). To what extent does this re-evaporation contribute to the  
288 atmospheric POPs? The Clausius-Clapeyron (CC) equation can be used to assess this probability  
289 (Wania et al., 1998b). If a strong relationship is found between the partial pressure of atmospheric OCPs  
290 and the air temperature, this indicates that volatilization may occur. Otherwise, low temperature  
291 dependence will occur in the case of LRAT. In the present study, the results of the CC equation are  
292 summarized in Table S17. The correlation with temperature ( $p > 0.05$ , Table S17) for most chemicals was  
293 not significant, except for  $\alpha$ -HCH, which displayed a relatively lower correlation coefficient ( $R^2 = 0.29$ ,  
294  $p < 0.05$ , Table S17). This indicates that weak volatilization of  $\alpha$ -HCH from local surfaces at Nam Co  
295 may exist, while the re-evaporation of other chemicals is limited.

296 Enantiomers of chiral POPs have been used to distinguish the contribution of LRAT and  
297 re-volatilization of POPs from surfaces (Bidleman et al., 2012). For example, technical HCH contains  
298 the (+)- and (-)- $\alpha$ -HCH enantiomers in a racemic proportion (EF=0.5). Abiotic processes (transport,  
299 hydrolysis, and photolysis) do not favor either enantiomer, while only biological processes, such as,  
300 microbial degradation in soils and water, show enantioselectivity and will alter the EFs of  $\alpha$ -HCH (Ridal  
301 et al., 1997). Therefore, nearly racemic signatures usually indicate input from LRAT, while nonracemic  
302 signatures represent the influence of local microbial degradation. In the present study, both the  
303 enantiomeric signatures of  $\alpha$ -HCH in air and water were measured simultaneously from May to  
304 September. As shown in Figure 5a, all the lake water samples showed a selective depletion of  
305 (+)- $\alpha$ -HCH, with EFs ranging from 0.318 to 0.449. This has previously been reported for other cold  
306 oligotrophic water systems, such as the Arctic Ocean (EFs: 0.393–0.438) (Lohmann et al., 2009). From  
307 Figure 5a, we found that extensive enantioselective degradation occurred in June and July, which  
308 coincided with the bacterial bloom period (Figure 5b) (Liu et al., 2013). Law et al. (2001) suggested that



309 under low nutrient conditions, oligotrophic bacteria are able to use xenobiotic carbon sources, such as  
310  $\alpha$ -HCH. This implies that the Tibetan lake microbes can also metabolize, or cometabolize,  $\alpha$ -HCH.

311 If high temperatures favor the evaporation of  $\alpha$ -HCH from the lake water, depletion of (+)- $\alpha$ -HCH  
312 should be observed for air. However, the EFs of the air samples were overall racemic. This is similar to  
313 the racemic composition observed in the atmosphere over Indian regions (Huang et al., 2013), which is  
314 the potential source region of HCHs in Nam Co. With respect to the enantiomeric signature in air  
315 samples from June and July, only some (+)  $\alpha$ -HCH depletion was observed in air (Figure 5a), indicating  
316 weak evaporation of  $\alpha$ -HCH from the lake water. Combined with the EF values in air and water, the  
317 fraction of the contribution from lake water volatilization ( $f$ ) can be quantified by (Huang et al., 2013):

$$318 \quad f = (EF_a - EF_b) / (EF_w - EF_b) \quad (8)$$

319 where  $EF_a$  and  $EF_w$  are the EF values in air and water, respectively; and  $EF_b$  is the background EF value  
320 in air, which was assumed to be the average EF of the standard. The estimated results show that only 19%  
321 and 17% of atmospheric  $\alpha$ -HCH came from water volatilization in June and July, respectively,  
322 demonstrating that LRAT is indeed the major source (more than 80%) of  $\alpha$ -HCH. This result is in  
323 contrast with the conclusion of Xiao et al. (2010) that evaporation from Nam Co Lake largely  
324 contributed to the atmospheric  $\alpha$ -HCH concentration. In that study, both levels and enantiomeric  
325 signatures of  $\alpha$ -HCH in Nam Co lake water were absent.

### 326 **3.4 Atmospheric processes**

#### 327 **3.4.1 Air-water gas exchange**

328 Although some  $\alpha$ -HCH evaporation was recorded in June and July, the air-water exchange process  
329 during the entire ablation period is of great concern as this is the main season transferring pollutants  
330 between air and water. Fugacity ratios ( $f_w/f_a$ ) and net exchange fluxes ( $F_{AW}$ ,  $\text{ng m}^{-2} \text{day}^{-1}$ ) were  
331 quantified using paired air-water samples collected from May to September in 2014. The average  
332 exchange status (average of  $f_w/f_a$ ) for HCHs, HCB, PCB 28, and PAHs during the ablation period is  
333 illustrated in Figure 6. Because of DDTs, Ant and Fla were not quantified in the lake water (Table S9)  
334 and were therefore excluded from the discussion.  $\alpha$ - and  $\gamma$ -HCH had low  $f_w/f_a$  values ranging from 0.08  
335 to 0.15, and 0.02 to 0.08, respectively (Figure 6a). The low  $f_w/f_a$  ratio suggests that  $\alpha$ - and  $\gamma$ -HCH were  
336 overall prone to deposition from air to water during the ablation period. The deposition fluxes were  $-1.6$   
337  $\pm 0.4 \text{ ng m}^{-2} \text{day}^{-1}$  for  $\alpha$ -HCH and  $-1.0 \pm 0.2 \text{ ng m}^{-2} \text{day}^{-1}$  for  $\gamma$ -HCH, which are within the same order of  
338 magnitude as those reported for the Great Lakes (Khairy et al., 2014). Connected to the source of HCHs



339 discussed above, this result implies that the following LRAT-deposition event of HCHs occurred in the  
340 ablation period of Nam Co Lake. In terms of  $\beta$ -HCH, PCB 28, and HCB, their  $f_w/f_a$  ratios overlapped  
341 with the equilibrium range but were on the edge of the deposition threshold ( $f_w/f_a = 0.3$ ). Therefore, low  
342 deposition fluxes for  $\beta$ -HCH ( $-0.2 \text{ ng m}^{-2} \text{ day}^{-1}$ ) and PCB 28 ( $-0.1 \text{ ng m}^{-2} \text{ day}^{-1}$ ), and large variability for  
343 HCB ( $-1.0 \pm 0.6 \text{ ng m}^{-2} \text{ day}^{-1}$ ) were observed (Figure 7a).

344 The results of the air-water gas exchange for PAHs are presented in Figure 6b. The fugacity ratios of  
345 thirteen PAHs varied depending on their molecular weight and volatility (Figure 6b). AceI and Ace  
346 showed  $f_w/f_a$  values significantly higher than 3 (Figure 6b), indicating that the lake acted as a secondary  
347 source for these volatile chemicals. In addition, Flu was close to equilibrium but showed a tendency  
348 toward volatilization to the air. The  $f_w/f_a$  values for Phe covered a large range (from 0.3 to 3), showing a  
349 shift between volatilization and deposition (Figure 6b). Other high molecular weight ( $MW > 202$ ) PAHs,  
350 including Pyr, BaA, Chr, Bbf, Bkf, Bap, IcdP, DahA, and BghiP, favored net deposition with  $f_w/f_a$   
351 values lower than 0.3 (Figure 6b). Greater volatilization fluxes were observed for AceI, Ace, and Flu  
352 (3-ring), which could reach up to  $203 \text{ ng m}^{-2} \text{ day}^{-1}$  (Figure 7b). Whereas, the gaseous deposition fluxes  
353 for high molecular weight PAHs were two orders of magnitudes lower and only varied from  $-1.0$  to  $-4.6$   
354  $\text{ng m}^{-2} \text{ day}^{-1}$  (Figure 7c). Although average deposition fluxes of  $339 \text{ ng m}^{-2} \text{ day}^{-1}$  were calculated for  
355 Phe, the deposition fluxes showed large variability ( $\pm 604 \text{ ng m}^{-2} \text{ day}^{-1}$ ). This result is broadly consistent  
356 with the exchange direction revealed by the  $f_w/f_a$  values, implying that the exchange of Phe between air  
357 and water may be reversed during the entire ablation period.

### 358 3.4.2 Reversal of the air-water exchange of Phe

359 In section 3.4.1, we observed that both the air-water exchange direction and the flux of Phe showed a  
360 large range of values and uncertainties. This raises a question about what drives this variation. The  
361 monthly calculated  $f_w/f_a$  and  $F_{AW}$  of Phe during the ablation period showed that the volatilization of Phe  
362 occurred during May and June, but deposition begun in July, which represents a reversal (Figure 8).  
363 Given that lake ice begins melting during May, the melted ice may discharge large amounts of  
364 accumulated PAHs into the lake, causing the relative enrichment (high fugacity) of Phe in the water, and  
365 triggering the secondary emission of Phe from the water to the atmosphere. This was confirmed by the  
366 increased water concentration of Phe found during May and June (Table S9). This is also the reason  
367 why a large uncertainty of  $F_{AW}$  was observed for Phe during the ablation period. Linked to the source of  
368 PAHs discussed above, the final exchange status of PAHs is the combined effects of the depositional  
369 input caused by biomass burning, the properties of the chemical, and the melting of lake ice.



370 Seasonal ice cover is an important feature of water bodies in cold regions. In the Arctic region, Jantunen  
371 et al. (2008) and Wong et al. (2011) both observed the occurrence of volatilization of POPs from  
372 seawater coincident with the breaking up of ice cover in the summer. The Nam Co Lake also undergoes  
373 long periods of ice-cover (Liu et al., 2013). During the winter, the lake surface is covered by ice and gas  
374 exchange is restricted, meanwhile dry and wet deposition exerts a significant influence on the input  
375 inventory of PAHs to the lake. Both of these two deposition processes are one-way (no volatilization),  
376 which keeps the contaminants being accumulated. As summer arrives, the lake ice begins to thaw and  
377 air-water gas exchange begins to dominate. On the one hand, after the higher accumulation of  
378 deposition, supersaturation of PAHs in the lake may occur. On the other hand, the fugacity capacity of  
379 ice is much higher than that of water, and therefore the decrease of the fugacity capacity during melting  
380 will increase the fugacity of the PAHs (Wania et al., 1998c), which also promotes their re-emission from  
381 the water. Although the seasonal ice cover did not show any obvious influence on the fate of OCPs and  
382 other PAHs, it played an important role in the fate of Phe, which was a dominant compound in the Nam  
383 Co atmosphere. The lake therefore acted as a secondary source of Phe in May and June, and shifted to a  
384 net sink during other months, which is likely driven by the seasonal freeze-thaw cycle of lake ice  
385 (Figure 8).

### 386 3.4.3 Atmospheric degradation

387 Reactions with the hydroxyl radical (OH) are an important removal process of gaseous POPs from the  
388 atmosphere. The resulting degradation fluxes ( $F_{\text{deg}}$ ,  $\text{ng m}^{-2} \text{day}^{-1}$ ) are dependent on the concentration of  
389 OH radicals in the air (Spivakovsky et al., 2000) and the compound-specific degradation rate constant  
390 ( $K_{\text{OH}}$ ,  $\text{cm}^3 \text{molecules}^{-1} \text{day}^{-1}$ ). The  $K_{\text{OH}}$  values of gaseous OCPs and PAHs are from Brubaker and Hites  
391 (1998) and Keyte et al. (2013), respectively. Due to the lack of information on  $K_{\text{OH}}$  for  $\beta$ -HCH and BaA,  
392 their degradation fluxes ( $F_{\text{deg}}$ ) were not considered in this study. The calculated  $F_{\text{deg}}$  values were  
393 averaged for individual POPs and are presented in Figure S4. The degradation fluxes for  $\alpha$ -,  $\gamma$ -HCH,  
394 HCB, and PCB 28 ranged between 0.3 and 0.9  $\text{pg m}^{-2} \text{day}^{-1}$  (Figure S4), 3 orders of magnitude lower  
395 than their  $F_{\text{AW}}$ . This indicates that the contribution of atmospheric degradation to their total inventory in  
396 the environment is negligible.

397 In contrast to the OCPs, the PAHs are more susceptible to photodegradation (Lohmann et al., 2009). In  
398 our study, lower molecular weight PAHs showed higher degradation fluxes, such as 4–184  $\text{ng m}^{-2} \text{day}^{-1}$   
399 for Phe, and 1–160  $\text{ng m}^{-2} \text{day}^{-1}$  for Ant (Figure S4). These values are similar to those reported for  $F_{\text{deg}}$   
400 in the remote atmosphere of the Atlantic Ocean (i.e., 7–120 and 9–50  $\text{ng m}^{-2} \text{day}^{-1}$  for Phe and Ant,



401 respectively) (Nizzetto et al., 2008). We observed relatively low  $F_{\text{deg}}$  values for 5- and 6-ring PAHs,  
402 ranging from 0.01 to 0.18  $\text{ng m}^{-2} \text{day}^{-1}$  (Figure S4). Generally, the  $F_{\text{deg}}$  of all PAH compounds was one  
403 order of magnitude lower than their  $F_{\text{AW}}$ . OH depletion is the primary process that removes atmospheric  
404 PAHs, presumably causing the continuous volatilization of low molecular weight PAHs from the water.  
405 This raised questions about other processes that may have supplied PAHs into the lake water. On the  
406 other hand, OH degradation also decreases the input of high molecular weight PAHs into the water and  
407 it is unclear to what extent this degradation counteracts other deposition processes.

#### 408 3.4.4 Atmospheric deposition

409 In addition to the gas exchange, dry and wet deposition are also important processes that influence the  
410 input of POPs from air to the lake. Dry ( $F_{\text{DD}}$ ) and wet ( $F_{\text{WD}}$ ) deposition was estimated using Equations  
411 4 and 6, respectively. With respect to HCHs, HCB, and PCB 28, their dry deposition fluxes ( $F_{\text{DD}}$ ) were  
412 negligible due to their low detection frequency in the particulate phase (Table S8). However, the  
413 average  $F_{\text{WD}}$  for  $\alpha$ -HCH,  $\beta$ -HCH, and  $\gamma$ -HCH was -0.3, -0.9, and -0.4  $\text{ng m}^{-2} \text{day}^{-1}$ , respectively, which  
414 is comparable to their  $F_{\text{AW}}$  levels.  $F_{\text{WD}}$  for HCB (-0.02  $\text{ng m}^{-2} \text{day}^{-1}$ ) and PCB 28 (-0.002  $\text{ng m}^{-2} \text{day}^{-1}$ )  
415 was two magnitudes lower than their  $F_{\text{AW}}$ . In general, precipitation scavenging is most efficient in  
416 HCHs compared with the other chemicals (Carrera et al., 2002). Greater wet deposition fluxes of HCHs  
417 occurred in August (Figure S5), coinciding with the highest amount of precipitation in Nam Co.  
418 Combining the  $F_{\text{AW}}$  and  $F_{\text{WD}}$  of HCHs, the estimated annual input of HCHs from air into the whole lake  
419 ( $2015 \text{ km}^2$ ) was 1.9  $\text{kg year}^{-1}$ . This result highlights the input of HCHs by the LRAT-deposition process  
420 during the ablation period (open water season). Snow scavenging of HCHs has been reported as an  
421 important clearing process in mountain regions (Kang et al., 2009). However, the transport of HCHs in  
422 winter is very limited due to the unfavorable air circulation patterns (westerly wind), ruling out the  
423 significant contribution of input of HCHs by snow scavenging.

424 Compared with OCPs, the close association between PAHs and the particulate phase accounted for their  
425 relatively higher deposition fluxes. The estimated dry and wet deposition fluxes for individual PAHs  
426 during the ablation and frozen periods, respectively, are provided in Table 1. We found that the  $F_{\text{DD}}$   
427 values of PAHs for the ablation period are, in general, lower than those for the frozen period. For  
428 example, the  $F_{\text{DD}}$  of total PAHs increased by one order of magnitude from the ablation period (4.5  $\text{ng}$   
429  $\text{m}^{-2} \text{day}^{-1}$ ) to the frozen period (38  $\text{ng m}^{-2} \text{day}^{-1}$ ; Table 1). Two factors may lead to the increase of  $F_{\text{DD}}$  in  
430 winter: the increased wind speed during the winter season and the growing particulate-PAH  
431 concentrations due to the enhanced combustion activities in winter. Compared with other studies, the



432 estimated  $F_{DD}$  for the total 15 PAHs ( $4.5\text{--}38\text{ ng m}^{-2}\text{ day}^{-1}$ , this study) is broadly within the range  
433 reported for global oceans ( $8.3\text{--}52.4\text{ ng m}^{-2}\text{ day}^{-1}$ ) (Gonzalez-Gaya et al., 2014).

434 Wet deposition was found to be the dominant deposition process for the input of PAHs into Nam Co  
435 (Table 1). This was expected because precipitation scavenging of organic chemicals underlies the  
436 accumulation of pollutants in mountain regions (Tremolada et al., 2008). In addition, there was an  
437 obvious difference between the values of  $F_{WD}$  during the ablation and frozen periods. For the total 15  
438 PAHs, the  $F_{WD}$  in the frozen period ( $702\text{ ng m}^{-2}\text{ day}^{-1}$ ) was approximately 5 times higher than that for  
439 the ablation period ( $161\text{ ng m}^{-2}\text{ day}^{-1}$ ), which may be due to the different precipitation types between  
440 these two periods (snow vs. rain). Snow has been suggested to be more efficient than rain for  
441 scavenging particulate-PAHs, which had a high concentration during winter in Nam Co (Table S8).  
442 Thus, although the precipitation of Nam Co in winter is low (less than 30 mm, Figure S2), the strong  
443 scavenging ratio of snow to PAHs combined with the relatively high particulate-PAHs concentration in  
444 winter caused the enhanced PAHs deposition in winter. The frozen season coincided with the period of  
445 high emission and high deposition of PAHs, implying a significant contribution of this season in the  
446 input of PAHs into the lake.

447 To calculate the comprehensive contribution of all above-mentioned processes, three groups of PAHs  
448 were classified in Table 1 based on their fate during the air-water exchange processes. PAHs (Acel, Ace,  
449 and Flu) showing volatilization behavior were placed into one group, PAHs with large  $F_{AW}$  variability  
450 between the status of volatilization and deposition were in the second group; and the remaining PAHs  
451 displaying deposition behavior were placed into the third group (Table 1). In this classification,  
452 although the air-water exchange direction and fluxes of Ant and Fla cannot be estimated, we still placed  
453 them into the second group because of their similarity to Phe in their physicochemical properties. For  
454 the volatilization group, the total outgassing from the lake was estimated to be approximately 126 kg  
455 per year, which cannot alone be supplied by their total deposition flux (sum of  $F_{WD}$  and  $F_{DD}$ ). This  
456 suggests that there may be additional natural sources of PAHs in the lake, such as, degradation of  
457 pigments carrying aromatic structure and turnover of organic matter (Nizzetto et al., 2008). Regarding  
458 the deposition group (Pyr, BaA, Chr, Bbf, Bkf, Bap, IcdP, DahA, and BghiP), their total deposition flux  
459 ( $F_{AW}+F_{DD}+F_{WD}$ ) will roughly cause the annual input of 208 kg high molecular weight PAHs into the  
460 lake. Although the  $F_{AW}$  of Phe was reversed and the total volatilization of Phe was estimated at around  
461  $26\text{ kg year}^{-1}$ , this loss will be complemented by the continuous deposition of Phe ( $\sim 373\text{ kg year}^{-1}$ ) from  
462 July to April. This indicates that the annual net input of Phe will be above 340 kg, which suggests that





463 Phe is the most dominant contributor in the total PAHs deposition. Considering the source of PAHs, the  
464 atmospheric deposition related to the regional biomass burning is assumed to be a potential  
465 anthropogenic carbon source to Nam Co Lake.

#### 466 **3.4.5 Uncertainties in flux estimation**

467 Several factors were involved in the uncertainties of the flux estimation: (i) loss during sample  
468 extraction and clean-up; (ii) measurement errors; and (iii) accuracy of the parameters in meteorology  
469 and physicochemical properties. The air-water gas exchange flux ( $F_{AW}$ ) is the most important  
470 contributor to the total inventory of PAHs into the lake. The uncertainty involved in  $F_{AW}$  was estimated  
471 by propagating the errors in  $C_a$  (30%),  $C_w$  (35%),  $K_{ol}$  (40%), and  $H$  (20%), which was 64%. These small  
472 errors demonstrate that the estimate of the gas exchange fluxes was relatively robust. By contrast, the  
473 confidence levels in the estimated  $F_{deg}$  and  $F_{WD}$  were a factor of 3–5, dominated by the uncertainty of  
474  $K_{OH}$ ,  $W_G$ , and  $W_P$  values for most PAHs in the study region. For example, the scavenging rates of PAHs  
475 by wet deposition were highly variable, which was caused by the complexity of the size distribution of  
476 aerosols, meteorological conditions, and the scavenging process (Jurado et al., 2005). Considering these  
477 aggregated uncertainties, the estimated fluxes here are only expected to capture the order of magnitude  
478 for the different processes. In addition, other input processes into the lake, such as, glacier meltwater,  
479 river runoff, and soil erosion may also occur in this study region, which will lead to an underestimation  
480 of the total input flux.

#### 481 **3.5 Implication for the regional carbon cycling**

482 Lakes are increasingly recognized as an important component of the terrestrial carbon cycle (Tranvik et  
483 al., 2009). Nearly 50% of the area of Chinese lakes is located on the TP, with general oligotrophic  
484 conditions and a total lake area of  $>43000 \text{ km}^2$  (Zhang et al., 2014). Compared with other components,  
485 such as grassland and forest, organic carbon burial in Tibetan lakes has been largely ignored. Although  
486 our study only focused on one of these lakes (Nam Co, area =  $2015 \text{ km}^2$ ), we can extrapolate the annual  
487 atmospheric deposition of PAHs into the remaining Tibetan lakes, and estimate it at 8.7 tons C, when  
488 expressed as carbon fluxes, which would become a significant allochthonous carbon source for these  
489 oligotrophic lakes. Because the Tibetan lakes are low in nutrients, bacteria in the lake have adapted to  
490 using a wide range of organic compounds and growing under starvation conditions (Liu et al., 2009).  
491 Recently, bacteria from the genus *Sphingomonas* were detected in Nam Co lake water and various  
492 glacier snows of the TP (Liu et al., 2013; Liu et al., 2009), and they were reported to have the ability to  
493 degrade PAHs (Leys et al., 2005). The presence of these bacteria in Nam Co suggests that the



494 atmospheric inputs of PAHs can act as a carbon source to support the survival of Tibetan microbial  
495 communities. Despite the natural PAH background in the environment, increasing biomass burning has  
496 led to the accumulation of PAHs in the lake sediments, especially during the past 50 years (Yang et al.,  
497 2016). Therefore, the continuous atmospheric deposition of PAHs and its ecological impact deserve  
498 greater concern.

#### 499 **4. Conclusions**

500 This study confirmed that the Nam Co Lake was still a net sink of HCHs, following the  
501 LRAT-deposition process, rather than a secondary source. By contrast, PAHs primarily originated from  
502 local biomass burning. Dominated by gas exchange and wet deposition, the air-water fluxes of PAHs to  
503 the whole Nam Co Lake were estimated to be 550 kg year<sup>-1</sup>, providing a substantial carbon source for  
504 the oligotrophic lake. Among the PAHs compounds, Phe showed a distinct behavior with monthly  
505 reversals of the air–water exchange, which was most likely driven by the seasonal melting of lake ice.  
506 This hypothesis requires further investigation, and a passive sampling technique is recommended as a  
507 viable alternative to enhance the spatial coverage of the investigation of air-water exchange in the TP.

508

#### 509 **Acknowledgments**

510 This study was supported by the National Natural Science Foundation of China (41671480, 41222010  
511 and 41571463) and Youth Innovation Promotion Association (CAS2011067). The authors would like to  
512 thank the staff at Nam Co Monitoring and Research Station for Multisphere Interactions for their help  
513 with the collection of field samples.

514 **References:**

- 515 Baek, S. Y., Choi, S. D., and Chang, Y. S.: Three-Year Atmospheric Monitoring of Organochlorine Pesticides and  
516 Polychlorinated Biphenyls in Polar Regions and the South Pacific, *Environ. Sci. Technol.*, 45, 4475-4482, doi:  
517 10.1021/Es1042996, 2011.
- 518 Bailey, R. E.: Global hexachlorobenzene emissions, *Chemosphere*, 43, 167-182, doi:Doi  
519 10.1016/S0045-6535(00)00186-7, 2001.
- 520 Bidleman, T. F., Jantunen, L. M., Kurt-Karakus, P. B., and Wong, F.: Chiral persistent organic pollutants as tracers of  
521 atmospheric sources and fate: review and prospects for investigating climate change influences, *Atmospheric*  
522 *Pollution Research*, 3, 371-382, doi: 10.5094/Apr.2012.043, 2012.
- 523 Brubaker, W. W., and Hites, R. A.: OH Reaction Kinetics of Gas-Phase  $\alpha$ - and  $\gamma$ -Hexachlorocyclohexane and  
524 Hexachlorobenzene, *Environ. Sci. Technol.*, 32, 766-769, 1998.
- 525 Carrera, G., Fernández, P., Grimalt, J. O., Ventura, M., Camarero, L., Catalan, J., Nickus, U., Thies, H., and Psenner, R.:  
526 Atmospheric deposition of organochlorine compounds to remote high mountain lakes of Europe, *Environ. Sci.*  
527 *Technol.*, 36, 2581-2588, 2002.
- 528 Cetin, B., Ozer, S., Sofuoglu, A., and Odabasi, M.: Determination of Henry's law constants of organochlorine  
529 pesticides in deionized and saline water as a function of temperature, *Atmos. Environ.*, 40, 4538-4546, doi:  
530 10.1016/j.atmosenv.2006.04.009, 2006.
- 531 Chakraborty, P., Zhang, G., Li, J., Sivakumar, A., and Jones, K. C.: Occurrence and sources of selected organochlorine  
532 pesticides in the soil of seven major Indian cities: Assessment of air-soil exchange, *Environ. Pollut.*, 204, 74-80,  
533 2015.
- 534 Dalla Valle, M., Jurado, E., Dachs, J., Sweetman, A. J., and Jones, K. C.: The maximum reservoir capacity of soils for  
535 persistent organic pollutants: implications for global cycling, *Environ. Pollut.*, 134, 153-164, doi:  
536 10.1016/j.envpol.2004.07.011, 2005.
- 537 Daly, G. L., Lei, Y. D., Teixeira, C., Muir, D. C. G., and Wania, F.: Pesticides in western Canadian mountain air and  
538 soil, *Environ. Sci. Technol.*, 41, 6020-6025, doi: 10.1021/Es070848o, 2007.
- 539 Ding, X., Wang, X. M., Xie, Z. Q., Xiang, C. H., Mai, B. X., Sun, L. G., Zheng, M., Sheng, G. Y., Fu, J. M., and  
540 Poschl, U.: Atmospheric polycyclic aromatic hydrocarbons observed over the North Pacific Ocean and the Arctic  
541 area: Spatial distribution and source identification, *Atmos. Environ.*, 41, 2061-2072,  
542 doi:10.1016/j.atmosenv.2006.11.002, 2007.
- 543 Fernandez, P., Grimalt, J. O., and Vilanova, R. M.: Atmospheric gas-particle partitioning of polycyclic aromatic  
544 hydrocarbons in high mountain regions of Europe, *Environ. Sci. Technol.*, 36, 1162-1168, doi: 10.1021/Es010190t,  
545 2002.
- 546 Franz, T. P., and Eisenreich, S. J.: Snow scavenging of polychlorinated biphenyls and polycyclic aromatic  
547 hydrocarbons in Minnesota, *Environ. Sci. Technol.*, 32, 1771-1778, doi: 10.1021/Es970601z, 1998.
- 548 Froescheis, O., Looser, R., Cailliet, G. M., Jarman, W. M., and Ballschmiter, K.: The deep-sea as a final global sink of  
549 semivolatile persistent organic pollutants? Part I: PCBs in surface and deep-sea dwelling fish of the North and  
550 South Atlantic and the Monterey Bay Canyon (California), *Chemosphere*, 40, 651-660, doi:  
551 10.1016/S0045-6535(99)00461-0, 2000.
- 552 Gioia, R., Lohmann, R., Dachs, J., Temme, C., Lakaschus, S., Schulz-Bull, D., Hand, I., and Jones, K. C.:  
553 Polychlorinated biphenyls in air and water of the North Atlantic and Arctic Ocean, *J. Geophys. Res.*, 113, doi:  
554 10.1029/2007jd009750, 2008.
- 555 Gioia, R., Li, J., Schuster, J., Zhang, Y. L., Zhang, G., Li, X. D., Spiro, B., Bhatia, R. S., Dachs, J., and Jones, K. C.:  
556 Factors Affecting the Occurrence and Transport of Atmospheric Organochlorines in the China Sea and the  
557 Northern Indian and South East Atlantic Oceans, *Environ. Sci. Technol.*, 46, 10012-10021, doi:  
558 10.1021/Es302037t, 2012.
- 559 Gong, P., Wang, X. P., and Yao, T. D.: Ambient distribution of particulate- and gas-phase n-alkanes and polycyclic



- 560 aromatic hydrocarbons in the Tibetan Plateau, *Environmental Earth Sciences*, 64, 1703-1711,  
561 doi:10.1007/s12665-011-0974-3, 2011.
- 562 Gonzalez-Gaya, B., Zuniga-Rival, J., Ojeda, M. J., Jimenez, B., and Dachs, J.: Field Measurements of the Atmospheric  
563 Dry Deposition Fluxes and Velocities of Polycyclic Aromatic Hydrocarbons to the Global Oceans, *Environ. Sci.*  
564 *Technol.*, 48, 5583-5592, doi:10.1021/es500846p, 2014.
- 565 Gonzalez-Gaya, B., Fernandez-Pinos, M. C., Morales, L., Mejanelle, L., Abad, E., Pina, B., Duarte, C. M., Jimenez, B.,  
566 and Dachs, J.: High atmosphere-ocean exchange of semivolatile aromatic hydrocarbons, *Nature Geoscience*, 9,  
567 438-442, doi:10.1038/NGEO2714, 2016.
- 568 Guglielmo, F., Stemmler, I., and Lammel, G.: The impact of organochlorines cycling in the cryosphere on their global  
569 distribution and fate-1. Sea ice, *Environ. Pollut.*, 162, 475-481, doi:10.1016/j.envpol.2011.09.039, 2012.
- 570 Guzzella, L., Poma, G., De Paolis, A., Roscioli, C., and Viviano, G.: Organic persistent toxic substances in soils,  
571 waters and sediments along an altitudinal gradient at Mt. Sagarmatha, Himalayas, Nepal, *Environ. Pollut.*, 159,  
572 2552-2564, doi:10.1016/j.envpol.2011.06.015, 2011.
- 573 Harner, T., Wiberg, K., and Norstrom, R.: Enantiomer fractions are preferred to enantiomer ratios for describing chiral  
574 signatures in environmental analysis, *Environ. Sci. Technol.*, 34, 218-220, 2000.
- 575 Hu, T., Cao, J., Lee, S., Ho, K., Li, X., Liu, S., and Chen, J.: Physiochemical characteristics of indoor PM<sub>2.5</sub> with  
576 combustion of dried yak dung as biofuel in Tibetan Plateau, China, *Indoor & Built Environment*, 191, 172-181,  
577 2015.
- 578 Huang, Y. M., Xu, Y., Li, J., Xu, W. H., Zhang, G., Cheng, Z. N., Liu, J. W., Wang, Y., and Tian, C. G.: Organochlorine  
579 Pesticides in the Atmosphere and Surface Water from the Equatorial Indian Ocean: Enantiomeric Signatures,  
580 Sources, and Fate, *Environ. Sci. Technol.*, 47, 13395-13403, doi: 10.1021/Es403138p, 2013.
- 581 Hung, H., Kallenborn, R., Breivik, K., Su, Y. S., Brorstrom-Lunden, E., Olafsdottir, K., Thorlacius, J. M., Leppanen, S.,  
582 Bossi, R., Skov, H., Mano, S., Patton, G. W., Stern, G., Sverko, E., and Fellin, P.: Atmospheric monitoring of  
583 organic pollutants in the Arctic under the Arctic Monitoring and Assessment Programme (AMAP): 1993-2006,  
584 *Sci. Total Environ.*, 408, 2854-2873, doi: 10.1016/j.scitotenv.2009.10.044, 2010.
- 585 Iwata, H., Tanabe, S., Sakai, N., and Tatsukawa, R.: Distribution of Persistent Organochlorines in the Oceanic Air and  
586 Surface Seawater and the Role of Ocean on Their Global Transport and Fate, *Environ. Sci. Technol.*, 27,  
587 1080-1098, 1993.
- 588 Jantunen, L. M., Helm, P. A., Kylin, H., and Bidlemant, T. F.: Hexachlorocyclohexanes (HCHs) in the Canadian  
589 archipelago. 2. Air-water gas exchange of alpha- and gamma-HCH, *Environ. Sci. Technol.*, 42, 465-470, doi:  
590 10.1021/Es071646v, 2008.
- 591 Jantunen, L. M., Wong, F., Gawor, A., Kylin, H., Helm, P. A., Stern, G. A., Strachan, W. M. J., Burniston, D. A., and  
592 Bidleman, T. F.: 20 Years of Air-Water Gas Exchange Observations for Pesticides in the Western Arctic Ocean,  
593 *Environ. Sci. Technol.*, 49, 13844-13852, doi:10.1021/acs.est.5b01303, 2015.
- 594 Jurado, E., Jaward, F., Lohmann, R., Jones, K. C., Simo, R., and Dachs, J.: Wet deposition of persistent organic  
595 pollutants to the global oceans, *Environ. Sci. Technol.*, 39, 2426-2435, doi: 10.1021/Es048599g, 2005.
- 596 Kang, J. H., Choi, S. D., Park, H., Baek, S. Y., Hong, S., and Chang, Y. S.: Atmospheric deposition of persistent  
597 organic pollutants to the East Rongbuk Glacier in the Himalayas, *Sci. Total Environ.*, 408, 57-63,  
598 doi:10.1016/j.scitotenv.2009.09.015, 2009.
- 599 Keyte, I. J., Harrison, R. M., and Lammel, G.: Chemical reactivity and long-range transport potential of polycyclic  
600 aromatic hydrocarbons - a review, *Chemical Society Reviews*, 42, 9333-9391, doi:10.1039/c3cs60147a, 2013.
- 601 Khairy, M., Muir, D., Teixeira, C., and Lohmann, R.: Spatial Trends, Sources, and Air-Water Exchange of  
602 Organochlorine Pesticides in the Great Lakes Basin Using Low Density Polyethylene Passive Samplers, *Environ.*  
603 *Sci. Technol.*, 48, 9315-9324, doi:10.1021/es501686a, 2014.
- 604 Komprda, J., Komprdova, K., Sanka, M., Mozny, M., and Nizzetto, L.: Influence of Climate and Land Use Change on  
605 Spatially Resolved Volatilization of Persistent Organic Pollutants (POPs) from Background Soils, *Environ. Sci.*  
606 *Technol.*, 47, 7052-7059, doi:10.1021/es30437134, 2013.



- 607 Kurt-Karakus, P. B., Bidleman, T. F., Staebler, R. M., and Jones, K. C.: Measurement of DDT fluxes from a historically  
608 treated agricultural soil in Canada, *Environ. Sci. Technol.*, 40, 4578-4585, doi: 10.1021/Es060216m, 2006.
- 609 Law, S. A., Diamond, M. L., Helm, P. A., Jantunen, L. M., and Alaei, M.: Factors affecting the occurrence and  
610 enantiomeric degradation of hexachlorocyclohexane isomers in northern and temperate aquatic systems, *Environ.*  
611 *Toxicol. Chem.*, 20, 2690-2698, 2001.
- 612 Leys, N. M., Ryngaert, A., Bastiaens, L., Top, E. M., Verstraete, W., and Springael, D.: Culture Independent Detection  
613 of *Sphingomonas* sp. EPA 505 Related Strains in Soils Contaminated with Polycyclic Aromatic Hydrocarbons  
614 (PAHs), *Microb. Ecol.*, 49, 443-450, 2005.
- 615 Li, C. L., Kang, S. C., Chen, P. F., Zhang, Q. G., and Fang, G. C.: Characterizations of particle-bound trace metals and  
616 polycyclic aromatic hydrocarbons (PAHs) within Tibetan tents of south Tibetan Plateau, China, *Environ Sci Pollut*  
617 *Res*, 19, 1620-1628, doi:10.1007/s11356-011-0678-y, 2012.
- 618 Li, C. L., Bosch, C., Kang, S. C., Andersson, A., Chen, P. F., Zhang, Q. G., Cong, Z. Y., Chen, B., Qin, D. H., and  
619 Gustafsson, O.: Sources of black carbon to the Himalayan-Tibetan Plateau glaciers, *Nature Communications*, 7,  
620 doi: 10.1038/Ncomms12574, 2016.
- 621 Li, J., Zhu, T., Wang, F., Qiu, X. H., and Lin, W. L.: Observation of organochlorine pesticides in the air of the Mt.  
622 Everest region, *Ecotoxicol. Environ. Saf.*, 63, 33-41, doi: 10.1016/j.ecoenv.2005.04.001, 2006.
- 623 Liu, X., and Chen, B.: Climatic warming in the Tibetan Plateau during recent decades, *International Journal of*  
624 *Climatology*, 20, 1729-1742, 2000.
- 625 Liu, X. B., Yao, T. D., Kang, S. C., Jiao, N. A. Z., Zeng, Y. H., and Liu, Y. Q.: Bacterial Community of the Largest  
626 Oligosaline Lake, Namco on the Tibetan Plateau, *Geomicrobiol. J.*, 27, 669-682, doi:  
627 10.1080/01490450903528000, 2010.
- 628 Liu, Y. Q., Yao, T. D., Jiao, N. Z., Kang, S. C., Xu, B. Q., Zeng, Y. H., Huang, S. J., and Liu, X. B.: Bacterial diversity  
629 in the snow over Tibetan Plateau Glaciers, *Extremophiles*, 13, 411-423, doi:10.1007/s00792-009-0227-5, 2009.
- 630 Liu, Y. Q., Yao, T. D., Jiao, N. Z., Liu, X. B., Kang, S. C., and Luo, T. W.: Seasonal Dynamics of the Bacterial  
631 Community in Lake Namco, the Largest Tibetan Lake, *Geomicrobiol. J.*, 30, 17-28,  
632 doi:10.1080/01490451.2011.638700, 2013.
- 633 Lohmann, R., Gioia, R., Jones, K. C., Nizzetto, L., Temme, C., Xie, Z., Schulz-Bull, D., Hand, I., Morgan, E., and  
634 Jantunen, L.: Organochlorine Pesticides and PAHs in the Surface Water and Atmosphere of the North Atlantic and  
635 Arctic Ocean, *Environ. Sci. Technol.*, 43, 5633-5639, doi: 10.1021/Es901229k, 2009.
- 636 Ma, J. M., Hung, H. L., Tian, C., and Kallenborn, R.: Revolatilization of persistent organic pollutants in the Arctic  
637 induced by climate change, *Nature Climate Change*, 1, 255-260, doi: 10.1038/Nclimate1167, 2011.
- 638 Ma, Y. G., Lei, Y. D., Xiao, H., Wania, F., and Wang, W. H.: Critical Review and Recommended Values for the  
639 Physical-Chemical Property Data of 15 Polycyclic Aromatic Hydrocarbons at 25 degrees C, *J. Chem. Eng. Data.*,  
640 55, 819-825, doi: 10.1021/Je900477x, 2010.
- 641 Ma, Y. X., Xie, Z. Y., Yang, H. Z., Moller, A., Halsall, C., Cai, M. H., Sturm, R., and Ebinghaus, R.: Deposition of  
642 polycyclic aromatic hydrocarbons in the North Pacific and the Arctic, *J. Geophys. Res.*, 118, 5822-5829,  
643 doi:10.1002/jgrd.50473, 2013.
- 644 Mulder, M. D., Heil, A., Kukucka, P., Klanova, J., Kuta, J., Prokes, R., Sprovieri, F., and Lammel, G.: Air-sea  
645 exchange and gas-particle partitioning of polycyclic aromatic hydrocarbons in the Mediterranean, *Atmospheric*  
646 *Chemistry and Physics*, 14, 8905-8915, doi:10.5194/acp-14-8905-2014, 2014.
- 647 Nizzetto, L., Lohmann, R., Gioia, R., Jahnke, A., Temme, C., Dachs, J., Herckes, P., Di, G. A., and Jones, K. C.: PAHs  
648 in air and seawater along a North-South Atlantic transect: trends, processes and possible sources, *Environ. Sci.*  
649 *Technol.*, 42, 1580-1585, 2008.
- 650 Noyes, P. D., McElwee, M. K., Miller, H. D., Clark, B. W., Van Tiem, L. A., Walcott, K. C., Erwin, K. N., and Levin, E.  
651 D.: The toxicology of climate change: Environmental contaminants in a warming world, *Environ. Int.*, 35,  
652 971-986, doi:10.1016/j.envint.2009.02.006, 2009.
- 653 Ridal, J. J., Bidleman, T. F., Kerman, B. R., Fox, M. E., and Strachan, W. M. J.: Enantiomers of



- 654 alpha-hexachlorocyclohexane as tracers of air-water gas exchange in Lake Ontario, *Environ. Sci. Technol.*, 31,  
655 1940-1945, doi: 10.1021/Es9607244, 1997.
- 656 Ruge, Z., Muir, D., Helm, P., and Lohmann, R.: Concentrations, Trends, and Air-Water Exchange of PAHs and PBDEs  
657 Derived from Passive Samplers in Lake Superior in 2011, *Environ. Sci. Technol.*, 49, 13777-13786,  
658 doi:10.1021/acs.est.5b02611, 2015.
- 659 Ruzickova, P., Klanova, J., Cupr, P., Lammel, G., and Holoubek, I.: An assessment of air-soil exchange of  
660 polychlorinated biphenyls and organochlorine pesticides across Central and Southern Europe, *Environ. Sci.*  
661 *Technol.*, 42, 179-185, doi: 10.1021/Es071406f, 2008.
- 662 Sheng, J. J., Wang, X. P., Gong, P., Joswiak, D. R., Tian, L. D., Yao, T. D., and Jones, K. C.: Monsoon-driven transport  
663 of organochlorine pesticides and polychlorinated biphenyls to the tibetan plateau: three year atmospheric  
664 monitoring study, *Environ. Sci. Technol.*, 47, 3199-3208, doi:10.1021/es305201s, 2013.
- 665 Spivakovsky, C. M., Logan, J. A., Montzka, S. A., Balkanski, Y. J., Foreman-Fowler, M., Jones, D. B. A., Horowitz, L.  
666 W., Fusco, A. C., Brenninkmeijer, C. A. M., and Prather, M. J.: Three-dimensional climatological distribution of  
667 tropospheric OH: Update and evaluation, *Journal of Geophysical Research Atmospheres*, 105, 8931-8980, 2000.
- 668 Stemmler, I., and Lammel, G.: Cycling of DDT in the global environment 1950-2002: World ocean returns the  
669 pollutant, *Geophys. Res. Lett.*, 36, doi:10.1029/2009GL041340, 2009.
- 670 Su, Y. S., Hung, H., Blanchard, P., Patton, G. W., Kallenborn, R., Konoplev, A., Fellin, P., Li, H., Geen, C., Stern, G.,  
671 Rosenberg, B., and Barrie, L. A.: A circumpolar perspective of atmospheric organochlorine pesticides (OCPs):  
672 Results from six Arctic monitoring stations in 2000-2003, *Atmos. Environ.*, 42, 4682-4698,  
673 doi:10.1016/j.atmosenv.2008.01.054, 2008.
- 674 Su, Y. S., Hung, H., Blanchard, P., Patton, G. W., Kallenborn, R., Konoplev, A., Fellin, P., Li, H., Geen, C., Stern, G.,  
675 Rosenberg, B., and Barrie, L. A.: Spatial and seasonal variations of hexachlorocyclohexanes (HCHs) and  
676 hexachlorobenzene (HCB) in the Arctic atmosphere, *Environ. Sci. Technol.*, 40, 6601-6607, doi:  
677 10.1021/Es061065q, 2006.
- 678 Tranvik, L. J., Downing, J. A., Cotner, J. B., Loiselle, S. A., Striegl, R. G., Ballatore, T. J., Dillon, P., Finlay, K.,  
679 Fortino, K., Knoll, L. B., Kortelainen, P. L., Kutser, T., Larsen, S., Laurion, I., Leech, D. M., McCallister, S. L.,  
680 McKnight, D. M., Melack, J. M., Overholt, E., Porter, J. A., Prairie, Y., Renwick, W. H., Roland, F., Sherman, B.  
681 S., Schindler, D. W., Sobek, S., Tremblay, A., Vanni, M. J., Verschoor, A. M., von Wachenfeldt, E., and  
682 Weyhenmeyer, G. A.: Lakes and reservoirs as regulators of carbon cycling and climate, *Limnol. Oceanogr.*, 54,  
683 2298-2314, doi: 10.4319/lo.2009.54.6\_part\_2.2298, 2009.
- 684 Tremolada, P., Villa, S., Bazzarin, P., Bizzotto, E., Comolli, R., and Vighi, M.: POPs in Mountain Soils from the Alps  
685 and Andes: Suggestions for a 'Precipitation Effect' on Altitudinal Gradients, *Water Air & Soil Pollution*, 188,  
686 93-109, 2008.
- 687 Venier, M., Dove, A., Romanak, K., Backus, S., and Hites, R.: Flame Retardants and Legacy Chemicals in Great  
688 Lakes' Water, *Environ. Sci. Technol.*, 48, 9563-9572, doi:10.1021/es501509r, 2014.
- 689 Vilanova, R. M., Fernandez, P., Martinez, C., and Grimalt, J. O.: Polycyclic aromatic hydrocarbons in remote mountain  
690 lake waters, *Water Res.*, 35, 3916-3926, doi: 10.1016/S0043-1354(01)00113-0, 2001.
- 691 Wang, C. F., Wang, X. P., Gong, P., and Yao, T. D.: Polycyclic aromatic hydrocarbons in surface soil across the Tibetan  
692 Plateau: Spatial distribution, source and air-soil exchange, *Environ. Pollut.*, 184, 138-144,  
693 doi:10.1016/j.envpol.2013.08.029, 2014.
- 694 Wang, J. B., Zhu, L. P., Daut, G., Ju, J. T., Lin, X., Wang, Y., and Zhen, X. L.: Investigation of bathymetry and water  
695 quality of Lake Nam Co, the largest lake on the central Tibetan Plateau, China, *Limnology*, 10, 149-158,  
696 doi:10.1007/s10201-009-0266-8, 2009.
- 697 Wang, X. P., Gong, P., Wang, C. F., Ren, J., and Yao, T. D.: A review of current knowledge and future prospects  
698 regarding persistent organic pollutants over the Tibetan Plateau, *Sci. Total Environ.*, 573, 139-154, doi:  
699 org/10.1016/j.scitotenv.2016.08.107, 2016.
- 700 Wang, X. P., Sheng, J. J., Gong, P., Xue, Y. G., Yao, T. D., and Jones, K. C.: Persistent organic pollutants in the Tibetan



- 701 surface soil: Spatial distribution, air-soil exchange and implications for global cycling, *Environ. Pollut.*, 170,  
702 145-151, doi: 10.1016/j.envpol.2012.06.012, 2012.
- 703 Wang, X. P., Gong, P., Sheng, J. J., Joswiak, D. R., and Yao, T. D.: Long-range atmospheric transport of particulate  
704 Polycyclic Aromatic Hydrocarbons and the incursion of aerosols to the southeast Tibetan Plateau, *Atmos.*  
705 *Environ.*, 115, 124-131, doi:10.1016/j.atmosenv.2015.04.050, 2015.
- 706 Wania, F., Axelman, J., and Broman, D.: A review of processes involved in the exchange of persistent organic  
707 pollutants across the air-sea interface, *Environ. Pollut.*, 102, 3-23, doi: 10.1016/S0269-7491(98)00072-4, 1998a.
- 708 Wania, F., Haugen, J. E., Lei, Y. D., and Mackay, D.: Temperature dependence of atmospheric concentrations of  
709 semivolatile organic compounds, *Environ. Sci. Technol.*, 32, 1013-1021, doi: 10.1021/Es970856c, 1998b.
- 710 Wania, F., Hoff, J. T., Jia, C. Q., and Mackay, D.: The effects of snow and ice on the environmental behaviour of  
711 hydrophobic organic chemicals, *Environ. Pollut.*, 102, 25-41, doi: 10.1016/S0269-7491(98)00073-6, 1998c.
- 712 Wilkinson, A. C., Kimpe, L. E., and Blais, J. M.: Air-water gas exchange of chlorinated pesticides in four lakes  
713 spanning a 1,205 meter elevation range in the Canadian Rocky Mountains, *Environ. Toxicol. Chem.*, 24, 61-69,  
714 doi: 10.1897/04-071r.1, 2005.
- 715 Wong, F., Jantunen, L. M., Pucko, M., Papakyriakou, T., Staebler, R. M., Stern, G. A., and Bidleman, T. F.: Air-Water  
716 Exchange of Anthropogenic and Natural Organohalogens on International Polar Year (IPY) Expeditions in the  
717 Canadian Arctic, *Environ. Sci. Technol.*, 45, 876-881, doi: 10.1021/Es1018509, 2011.
- 718 Xiao, H., Kang, S. C., Zhang, Q. G., Han, W. W., Loewen, M., Wong, F., Hung, H., Lei, Y. D., and Wania, F.: Transport  
719 of semivolatile organic compounds to the Tibetan Plateau: Monthly resolved air concentrations at Nam Co, *J.*  
720 *Geophys. Res.*, 115, doi: 10.1029/2010jd013972, 2010.
- 721 Xiao, Q. Y., Saikawa, E., Yokelson, R. J., Chen, P. F., Li, C. L., and Kang, S. C.: Indoor air pollution from burning yak  
722 dung as a household fuel in Tibet, *Atmos. Environ.*, 102, 406-412, doi:10.1016/j.atmosenv.2014.11.060, 2015.
- 723 Xie, Z., Koch, B. P., Moller, A., Sturm, R., and Ebinghaus, R.: Transport and fate of hexachlorocyclohexanes in the  
724 oceanic air and surface seawater, *Biogeosciences*, 8, 2621-2633, doi:10.5194/bg-8-2621-2011, 2011.
- 725 Yang, R. Q., Xie, T., An, L., Yang, H., Turner, S., Wu, G., and Jing, C.: Sedimentary records of polycyclic aromatic  
726 hydrocarbons (PAHs) in remote lakes across the Tibetan Plateau, *Environ. Pollut.*, 214, 1-7, 2016.
- 727 Yao, T. D., Thompson, L. G., Mosbrugger, V., Zhang, F., Ma, Y., Luo, T., Xu, B. Q., Yang, X., Joswiak, D. R., Wang,  
728 W., Joswiak, M. E., Devkota, L. P., Tayal, S., Jilani, R., and Fayziev, R.: Third Pole Environment (TPE),  
729 *Environmental Development*, 3, 52-64, doi:10.1016/j.envdev.2012.04.002, 2012.
- 730 Zhang, G., Chakraborty, P., Li, J., Sampathkumar, P., Balasubramanian, T., Kathiresan, K., Takahashi, S., Subramanian,  
731 A., Tanabe, S., and Jones, K. C.: Passive Atmospheric Sampling of Organochlorine Pesticides, Polychlorinated  
732 Biphenyls, and Polybrominated Diphenyl Ethers in Urban, Rural, and Wetland Sites along the Coastal Length of  
733 India, *Environ. Sci. Technol.*, 42, 8218-8223, doi: 10.1021/Es8016667, 2008.
- 734 Zhang, G. Q., Yao, T. D., Xie, H. J., Zhang, K. X., and Zhu, F. J.: Lakes' state and abundance across the Tibetan  
735 Plateau, *Chin. Sci. Bull.*, 59, 3010-3021, doi:10.1007/s11434-014-0258-x, 2014.
- 736 Zhang, W. L., Zhang, G., Qi, S. H. and Peng, P. A.: A preliminary study of organochlorinepesticides in water and  
737 sediments from two Tibetan Lakes. *Geochimica*. 32 (4), 363-367 (in Chinese with English abstract), 2003.

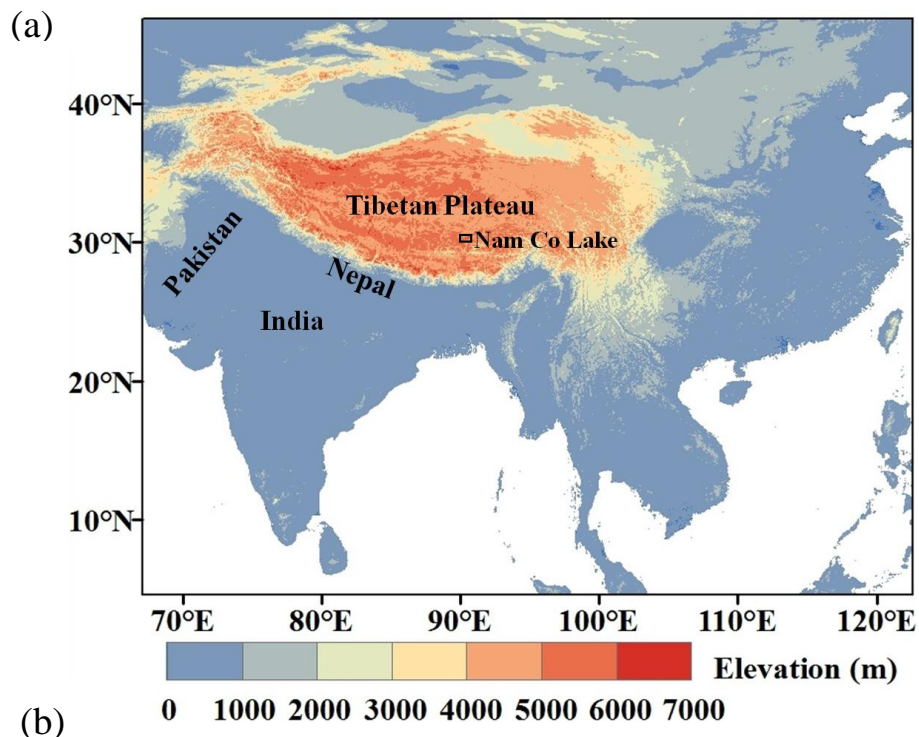


738 **Table 1. Estimated fluxes ( $\text{ng m}^{-2} \text{day}^{-1}$ ) of air-water gas exchange ( $F_{\text{AW}}$ ), atmospheric degradation ( $F_{\text{deg}}$ ), dry deposition ( $F_{\text{DD}}$ ), and**  
 739 **wet deposition ( $F_{\text{WD}}$ ) for individual PAHs during the ablation period and frozen periods, respectively.**

PAH	ablation period				PAH	frozen period		
	$F_{\text{AW}}$	$F_{\text{deg}}$	$F_{\text{DD}}$	$F_{\text{WD}}$		$F_{\text{deg}}$	$F_{\text{DD}}$	$F_{\text{WD}}$
<b>Volatilization compounds</b>								
Acel	$80 \pm 49$	$6 \pm 5$	NA	$-0.2 \pm 0.1$	Acel	$1 \pm 0.7$	$-0.02 \pm 0.001$	$-0.03 \pm 0.1$
Ace	$51 \pm 19$	$4 \pm 4$	$-0.003 \pm 0.002$	$-0.4 \pm 0.3$	Ace	$0.9 \pm 0.5$	$-0.01 \pm 0.01$	$-6 \pm 5$
Flu	$203 \pm 162$	$11 \pm 8$	$-0.1 \pm 0.02$	$-9 \pm 7$	Flu	$1.8 \pm 0.9$	$-0.2 \pm 0.2$	$-43 \pm 30$
<b>sum</b>	<b>335</b>	<b>21</b>	<b>-0.1</b>	<b>-9</b>	<b>sum</b>	<b>4</b>	<b>-0.2</b>	<b>-49</b>
Phe	$-340 \pm 604$	$82 \pm 67$	$-0.5 \pm 0.1$	$-42 \pm 35$	Phe	$10 \pm 4$	$-2.2 \pm 1.2$	$-345 \pm 237$
Ant	NA	$60 \pm 63$	$-0.04 \pm 0.03$	$-5 \pm 5$	Ant	$4 \pm 2$	$-0.11 \pm 0.05$	$-16 \pm 14$
Fla	NA	$5 \pm 5$	$-0.5 \pm 0.1$	$-20 \pm 18$	Fla	$0.5 \pm 0.3$	$-4.6 \pm 2.8$	$-93 \pm 64$
<b>Deposition compounds</b>								
Pyr	$-145 \pm 154$	$20 \pm 21$	$-0.4 \pm 0.1$	$-18 \pm 17$	Pyr	$2 \pm 1$	$-3 \pm 1.5$	$-128 \pm 83$
BaA	$-19 \pm 23$	NA	$-0.1 \pm 0.1$	$-3 \pm 4$	BaA	NA	$-1.1 \pm 0.5$	$-15 \pm 10$
Chr	$-54 \pm 62$	$7 \pm 8$	$-0.5 \pm 0.3$	$-47 \pm 56$	Chr	$0.2 \pm 0.1$	$-4.7 \pm 2.3$	$-19 \pm 13$
Bbf	$-5 \pm 3$	$0.2 \pm 0.1$	$-0.6 \pm 0.5$	$-6 \pm 5$	Bbf	$0.02 \pm 0.01$	$-2.2 \pm 3.2$	$-4 \pm 8$
Bkf	$-2 \pm 1$	$0.2 \pm 0.1$	$-0.4 \pm 0.4$	$-2 \pm 1$	Bkf	$0.1 \pm 0.04$	$-3.8 \pm 1.9$	$-8 \pm 5$
Bap	$-2 \pm 1$	$0.2 \pm 0.2$	$-0.3 \pm 0.5$	$-3 \pm 1$	Bap	$0.04 \pm 0.03$	$-4.7 \pm 2.3$	$-16 \pm 10$
IcdP	$-2 \pm 1$	$0.7 \pm 0.5$	NA	$-2 \pm 2$	IcdP	$0.1 \pm 0.1$	NA	$-3 \pm 6$
DahA	$-1 \pm 0.7$	$0.1 \pm 0.1$	NA	$-0.1 \pm 0.2$	DahA	$0.01 \pm 0.01$	NA	$-0.6 \pm 1$
BghiP	$-2 \pm 0.4$	$0.02 \pm 0.01$	$-1 \pm 1$	$-3 \pm 1$	BghiP	$0.01 \pm 0.01$	$-12 \pm 6$	$-6 \pm 3$
<b>sum</b>	<b>-231</b>	<b>28</b>	<b>-3</b>	<b>-85</b>	<b>sum</b>	<b>2</b>	<b>-31</b>	<b>-199</b>
<b>Total PAHs</b>	<b>\</b>	<b>196</b>	<b>-4.5</b>	<b>-161</b>	<b>Total PAHs</b>	<b>20</b>	<b>-38</b>	<b>-702</b>

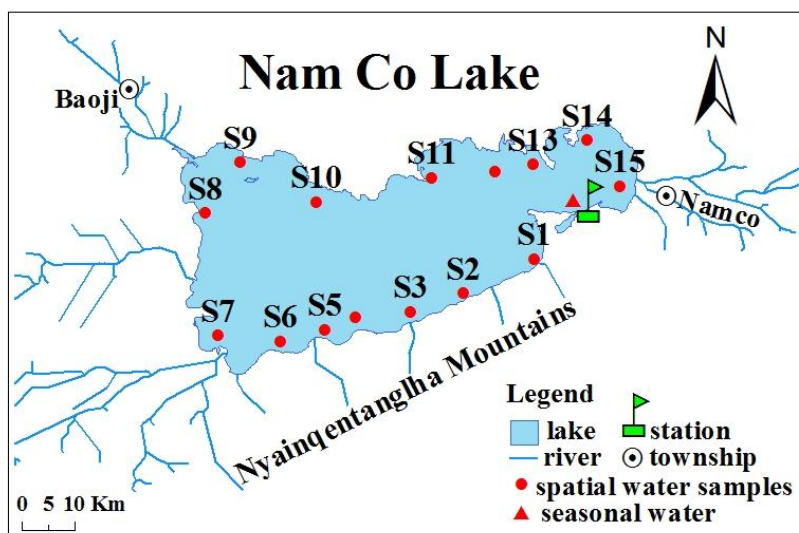
740 NA: not available; For  $F_{\text{AW}}$ ,  $F_{\text{DD}}$  and  $F_{\text{WD}}$ , positive values indicate volatilization, and negative values indicate net deposition.





741

(b)

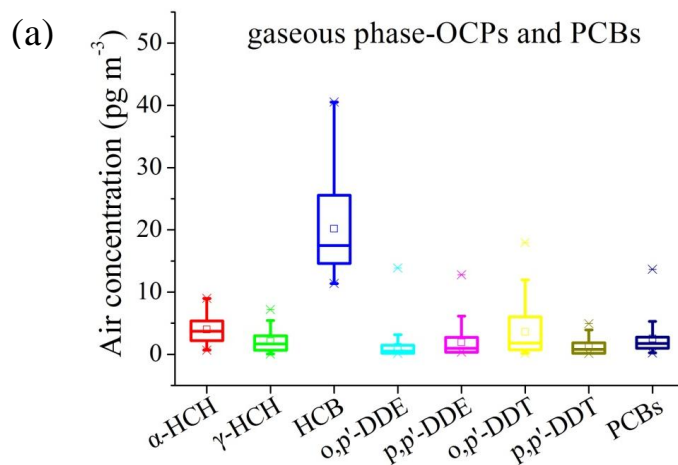


742

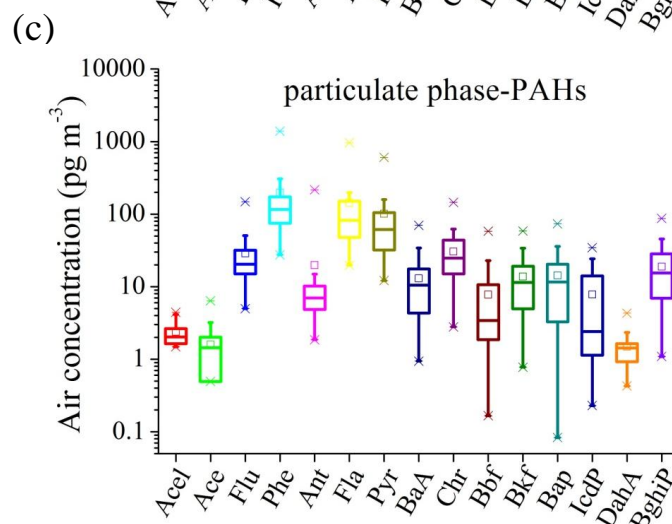
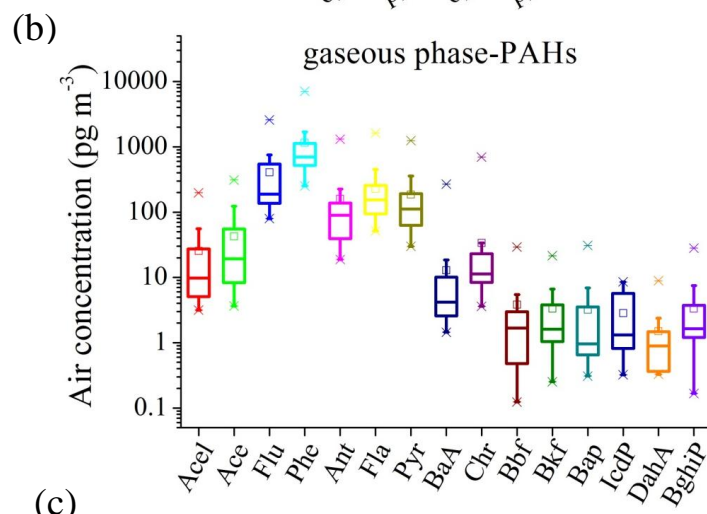
743 **Figure 1.** Location of Nam Co Lake on the Tibetan Plateau (a) and the sampling sites for air and  
744 lake water (b). The station refers to the Nam Co Monitoring and Research Station, and it is also  
745 the air sampling site; S01 to S15 represent the 15 sampling sites of surface water around the lake;  
746 the red triangle represents the sampling site of seasonal water from May to September.



747



748

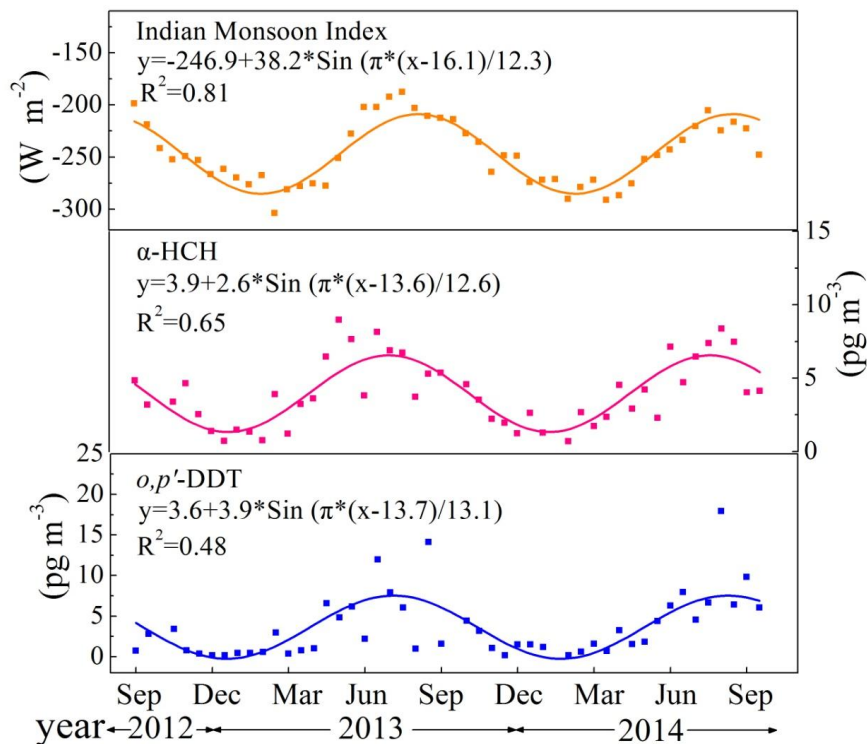


749

750 **Figure 2. Air concentrations of gaseous OCPs and PCBs (a), gaseous PAHs (b), and particulate**  
751 **phase PAHs (c) in Nam Co. The boxes are defined by the 25th and 75th percentiles; whiskers**  
752 **mark the 10th and 90th percentiles; the median is represented by a horizontal line; the mean by a**



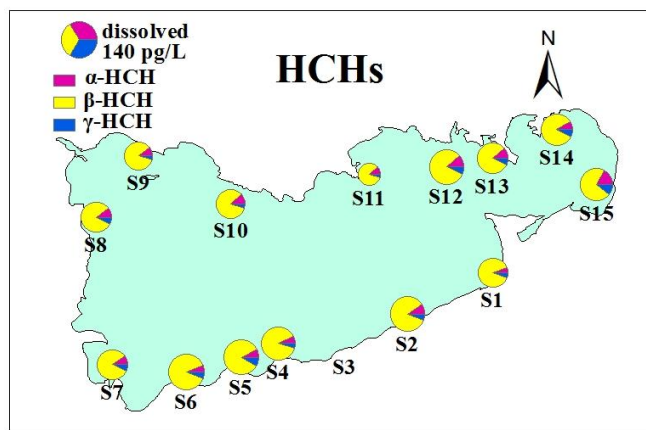
753 **square; and outliers with an asterisk.**



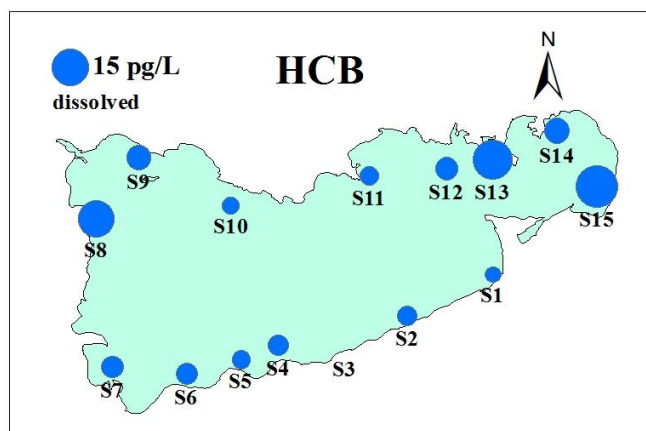
754

755 **Figure 3. Seasonal patterns of Indian Monsoon Index, the atmospheric concentrations of  $\alpha$ -HCH**

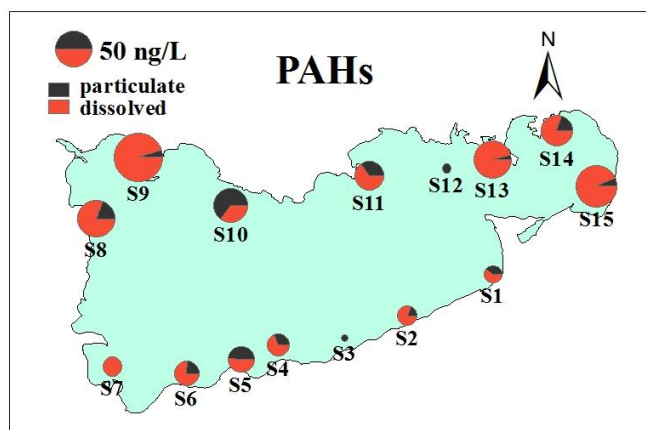
756 **and *o,p'*-DDT.**



757

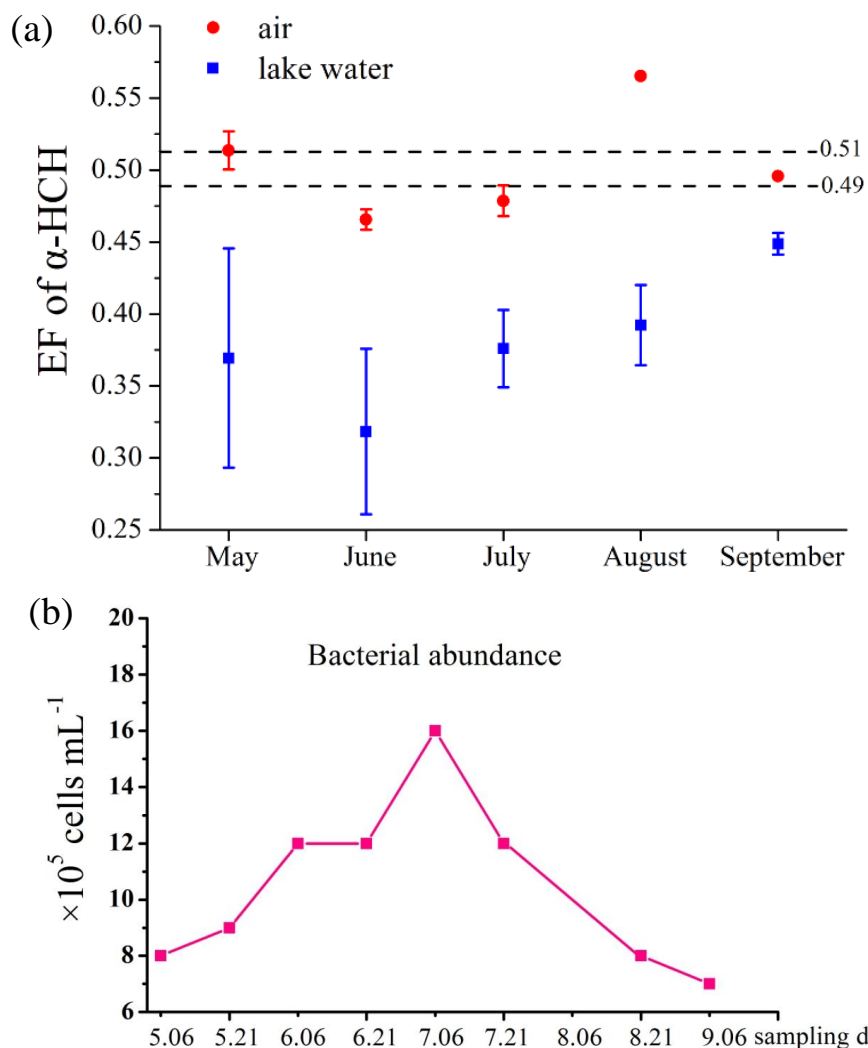


758



759

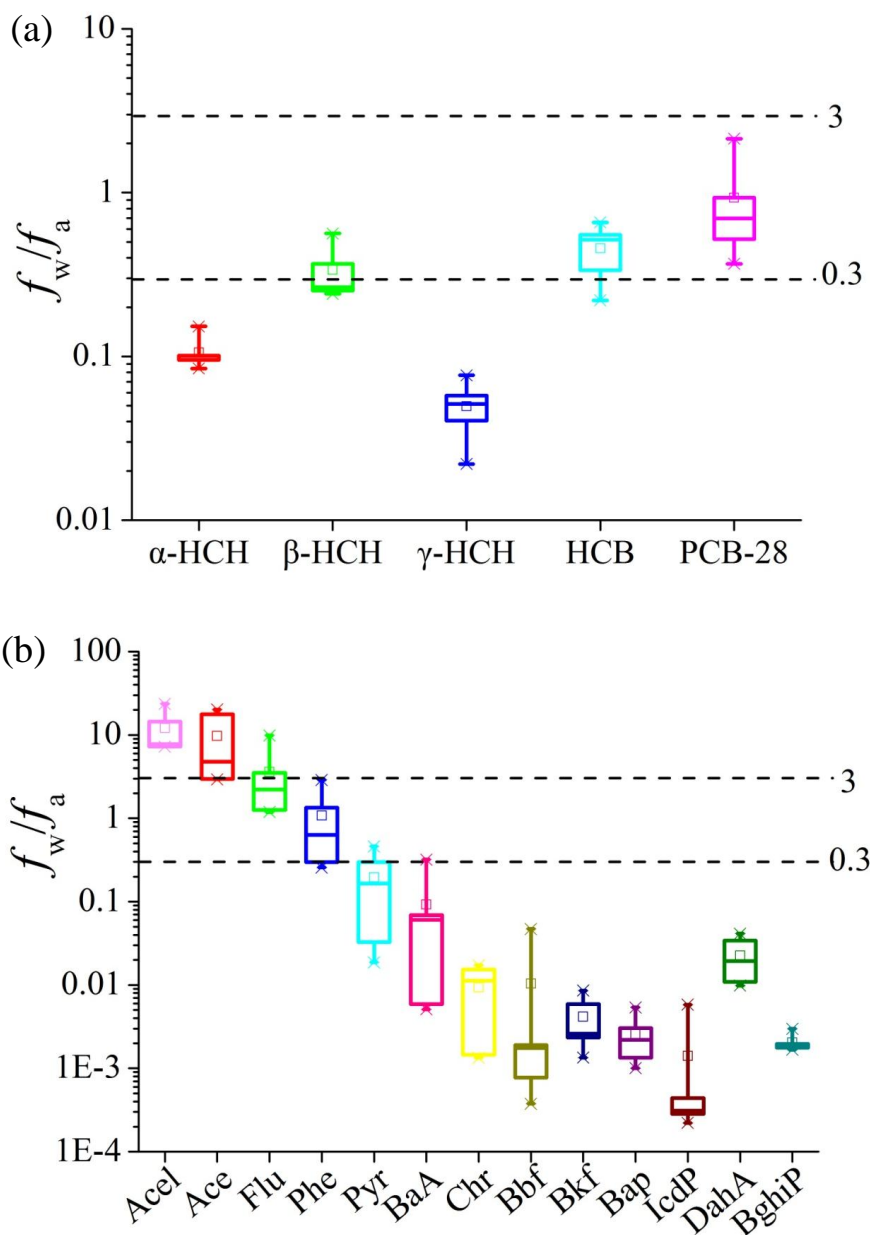
760 **Figure 4. Spatial distribution pattern of HCHs, HCB, and PAHs in the surface water of Nam Co**  
761 **Lake.**



762

763

764 **Figure 5. Enantiomer fraction (EF) of  $\alpha$ -HCH in the air and surface water from May to**  
765 **September (a), and the seasonal bacterial abundance in Nam Co Lake water (b). The data of**  
766 **bacterial abundance was derived from Liu et al. (2013), which represents the total bacteria in the**  
767 **lake surface water.**



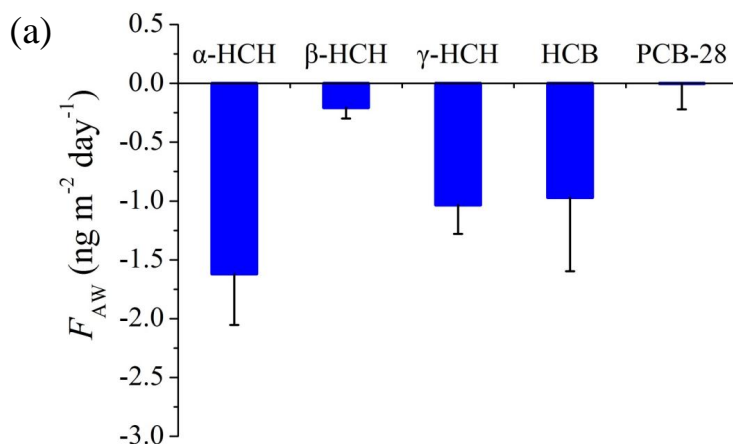
768

769

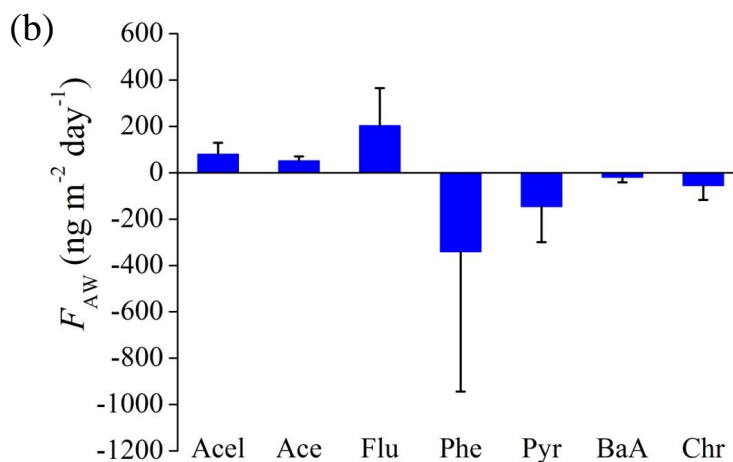
770 **Figure 6. Water/air fugacity ratios ( $f_w/f_a$ ) for OCPs and PCB 28 (a), and individual PAHs (b) in**  
771 **Nam Co Lake. The horizontal lines represent the uncertainty range, 0.3-3 was considered as**  
772 **equilibrium.**



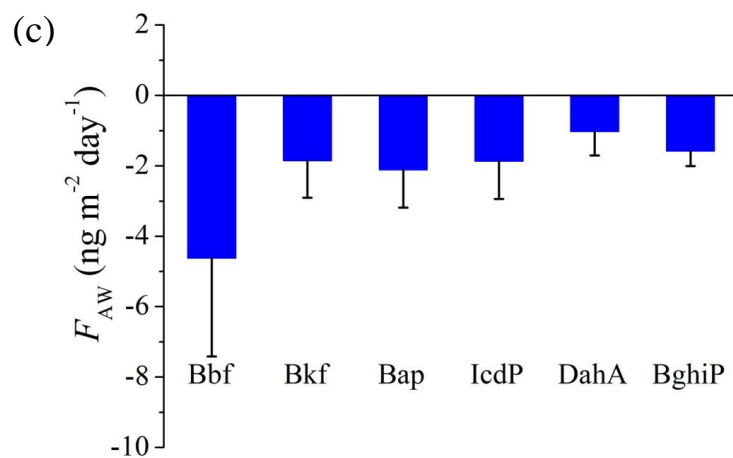
773



774

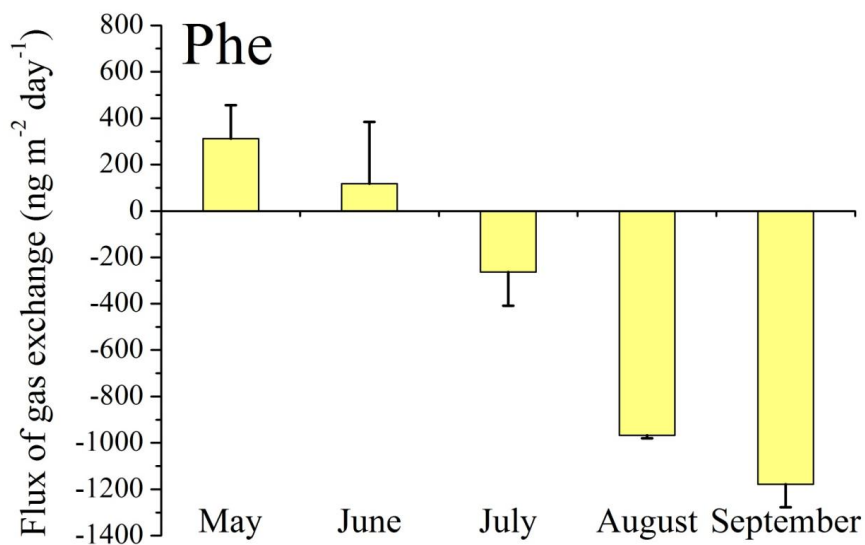


775



776 **Figure 7. Average air-water gas exchange fluxes ( $F_{AW}$ ) for individual OCPs, PCB 28 (a), and PAHs**  
777 **(b, c) in Nam Co Lake. Positive values indicate net volatilization, and negative values indicate net**  
778 **deposition.**





779

780 **Figure 8. Reversal of the air-water gas exchange for Phe from May to September.**